NTNU – Trondheim
Norwegian University of
Science and Technology

Oscillating foil propulsion

Jacob Hauge

Marine Technology
Submission date: August 2013
Supervisor: Sverre Steen, IMT

Norwegian University of Science and Technology
Department of Marine Technology

To my dear brother and friend, Andreas,

whom I love very much.

I know that my redeemer liveth,

and that He shall stand at the latter day upon the earth.

And though worms destroy this body,

yet in my flesh shall I see God.

Job 19,25-26

Scope of work

MASTER THESIS IN MARINE TECHNOLOGY

SPRING 2013

FOR

Jacob Hauge

Oscillating foil propulsion

One of the potential technologies for fuel saving of ships is to utilize wave power for propulsion. To utilize the relative vertical motions between water and ship to create thrust from foils attached to the ship is an old concept which has received renewed attention the last few years due to increasing bunker prices and increasing environmental concerns.
It has also been proposed to force motions on the foil in order to create thrust and propel the ship also in calm water. In this way, there is no need for a propeller at all. It might be possible to combine wave power and engine power, and propel the ship with a combination of supplied engine power and wave power in intermediate sea states.
The objective of the master thesis is to give an evaluation of the feasibility and efficiency of such a combined foil propulsion system.
To reach this objective, the candidate should:

- Present a summary of previous work in this field, in order to establish the state of the art.
- Establish and verify a simple simulation model for ship heave and pitch motions, initially for a ship alone, then extended to include a passive foil, and active foil(s). The simulation model shall be verified against independent calculations as far as possible.
- Establish a prediction model for the thrust, vertical force and required supplied power to a foil in forced oscillation in heave and pitch, at different forward speeds.
- Study the combination of a ship with one or more foils with forced oscillations in heave and pitch. The study shall consider issues such as efficiency, ship motions and accelerations, and foil forces.
- Discuss possible foil configurations and give recommendations for configurations.
- Consider the combination of incoming waves and forced motions, and investigate the potential for energy saving in different sea states and operational conditions.

In the thesis the candidate shall present his personal contribution to the resolution of problem within the scope of the thesis work.

Theories and conclusions should be based on mathematical derivations and/or logic reasoning identifying the various steps in the deduction.

The candidate should utilize the existing possibilities for obtaining relevant literature.

The thesis should be organized in a rational manner to give a clear exposition of results, assessments, and conclusions. The text should be brief and to the point, with a clear language. Telegraphic language should be avoided.

The thesis shall contain the following elements: A text defining the scope, preface, list of contents, summary, main body of thesis, conclusions with recommendations for further work, list of symbols and acronyms, reference and (optional) appendices. All figures, tables and equations shall be numerated.

The supervisor may require that the candidate, in an early stage of the work, present a written plan for the completion of the work. The plan should include a budget for the use of computer and laboratory resources that will be charged to the department. Overruns shall be reported to the supervisor.

The original contribution of the candidate and material taken from other sources shall be clearly defined. Work from other sources shall be properly referenced using an acknowledged referencing system.

The thesis shall be submitted in two copies:

1. Signed by the candidate
2. The text defining the scope included
3. In bound volume(s)
4. Drawings and/or computer prints that cannot be bound should be organized in a separate folder.
5. The bound volume shall be accompanied by a CD or DVD containing the written thesis in Word or PDF format. In case computer programs have been made as part of the thesis work, the source code shall be included. In case of experimental work, the experimental results shall be included in a suitable electronic format.

Supervisor : Professor Sverre Steen
Advisor : Eirik Bøckmann
Start : 14.01.2013
Deadline : 10.06.2013

Trondheim, 11.01.2013

Sverre Steen
Supervisor

Preface and acknowledgements

This report is the master thesis of Jacob Hauge completed in August 2013 at the Department of Marine Technology at NTNU, Trondheim. The project was supervised by professor Sverre Steen, and co-supervised by phd candidate Eirik Bøckmann. A great thanks to Sverre Steen for his patience and discussions. I also thank Eirik Bøckmann Morten Dinhoff Pedersen for taking the time to listen to my questions and debate with me. Thanks to Halvor Aga, Amund Ersland, my parents Maryse and Carl Christian Hauge and my brother Andreas for discussions and support.

Much time was spent understanding and developing theory. Application of the theory, however, proved more difficult than anticipated. Thus, not all parts of the task have been accounted for. The last task, investigating the potential for energy saving in different sea states, was dropped from the task in agreement with prof. Steen.

As Eitzen(2012), the author must conclude that the topic is challenging to approach.

Abstract

Unsteady foil theory is discussed and applied on several cases of an oscillating foil. The oscillating foil is meant as a propulsion system for a platform supply vessel.

Four case studies of foil oscillation have been performed. A thrust coefficient of 0.1 was achieved at an efficiency of 0.75. A thrust coefficient of minimum 0.184 is necessary to overcome the calm water resistance of the foil.

Issues connected to coupled vessel-foil models are discussed.

Sammendrag på norsk

Ikke-stasjonær foil teori blir drøftet og anvendt på flere studier av en oscillerende foil som er ment å brukes til fremdrift av en supplybåt.

Fire studier av foil oscillasjon ble utført. En thrustkoeffisient på 0.1 ble oppnådd med en virkningsgrad på 0.75. En koeffisient på minimum 0.184 er nødvendig for å overvinne stillevannsmotstanden til eksempelskipet anvendt her.

Anvendelser knyttet til koblede skip-foil-modeller blir drøftet.

Table of contents

List of figures

List of tables

Nomenclature and definitions

Symbols

A_F	Advance force of foil
A	Planform area of foil: projected of the foil on to the xy-plane or Added mass coefficient, generic
A_0	Constant term in viscous lift-drag polynomial
A_2	Constant multiplum of the second order term in the viscous lift-drag polynomial
a_{33F}	2D added mass coefficient of foil in heave
B	Damping coefficient
B_2	See definition on page 21
c	Chord length / mean chord length
C	Theodorsen function or Restoring coefficient
c_0	Chord length at center span
$C\left(k_f\right)$	Theodorsen function
C_{addF}	Added mass coefficient of foil
C_{adv}	Advance coefficient
C_D	Drag coefficient
C_{Dp}	Potential drag coefficient
C_{Du}	Unsteady drag coefficient
C_{Dv}	Viscous drag coefficient
C_L	Lift coefficient

C_{L0}	The factor relating α to C_L. Is 2π for 2D foils, and $\frac{2\pi}{1+2/\Lambda}$ for elliptical foils.
C_{Lu}	Unsteady lift coefficient. Equal to $C_L C\left(k_f\right)$
c_{mean}	Mean chord length
C_{res}	Foil resistance coefficient
C_T	Thrust coefficient
C_V	Foil vertical force coefficient
D	Drag force
F_{ex}	Excitation force
g	Gravitational acceleration $= 9.81\left[m/s^2\right]$
$h, \dot{h}, \ddot{h}$	Foil heave motion, velocity, acceleration
h_0	Foil heave amplitude
k	Wave number
K	Retardation function in Cummins equation
k_f	Reduced frequency
L	Lift force
M	Mass (of vessel)
R_F	Resistance force on foil
s	Foil span
$Se\left(k_f\right)$	Sears function
t	Time
T	Thrust force
U	Uniform velocity
V_A	Instantaneous inflow velocity
v_{rel}	Relative vertical velocity between foil and water , foil pitch angle included
$w, \dot{w}$	Vertical velocity/acceleration component of water particles in waves
x_f	X-location of foil
x_{rot}	Center of rotation of foil

$\dot{z}$	Relative vertical velocity between foil and water , foil pitch angle not included
$\ddot{z}$	Relative vertical acceleration between foil and water , foil pitch angle not included
z_f	Z-location of foil
α	Angle of attack
α_e	Effective angle of attack
α_{opt}	Optimal angle of attack
δ	Pitch angle of foil relative to horizontal plane
δ_0	Pitch angle amplitude
$\eta, \dot{\eta}, \ddot{\eta}$	Rigid body motion, velocity and acceleration of vessel
ρ	Density of water
λ	Wave length
Λ	Aspect ratio
γ	Local circulation distribution
Γ	Circulation
μ	Approximation of the fluid memory term in Cummins equation
σ	Foil efficiency
ω	Angular frequency [rad/s]
ω_0	Wave frequency
ω_e	Encounter frequency
φ	Angle between horizontal plane and effective incoming flow
ϕ	Wave potential
ϕ_e	Encounter potential
ζ_a	Wave amplitude

Table 1: Definition of symbols used in this report

Clarification:

A capital C with a subscript denotes a coefficient.
A capital C without any subscript denotes the Theodorsen function.
A lower case c denotes either a generic chord length or specifically the mean chord length of a 3D foil.

Acronyms

COG	Center of gravity
DOF	Degree of freedom
FD	Frequency domain
LE	Leading edge
RAO	Response amplitude operator
TD	Time domain
TE	Trailing edge

Table 2: Definition of acronyms used in this report

1 Introduction and state of the art

Oscillating foils provide a means of propulsion which has been known empirically since 1858 as far as can be documented.

The first theoretical analyses to “crack” the problem was performed by (Theodorsen 1934). Since then, analytical, numerical and experimental approaches to understanding oscillating foils have abounded, resulting in a perplexing variety of notation, perspectives and results.

Attempts to apply unsteady foil theory to vessel propulsion is less abundant. Some studies have been performed by e.g. (De Silva and Yamaguchi 2012) and (Naito and Isshiki 2005).

At the Department of Marine Technology at NTNU, several master projects have been published on the subject of oscillating foil propulsion. One phd candidate is currently studying the topic. The last years’ thesis have shown that the topic is quite advanced.

2 Mathematical tools

The terms and mathematical tools applied in this project may be familiar to the reader, but a certain clarification is deemed necessary in order to explain how the terms are used here.

2.1 Frequency domain

Linear dynamical systems that oscillate in time with a one-to-one relation between input and output frequency can be analyzed in the frequency domain. This implies that all terms in the equations include a time factor $e^{i\omega t}$ which can be eliminated, and the response amplitudes and phases may be solved for when the input amplitude and phases are defined. The state of the system at a certain point in time can be determined by multiplying the solution with $e^{i\omega t}$ and taking the real part of the value.

Frequency domain equations may be superimposed. I.e. assuming a linear system is oscillating simultaneously with several frequencies, the effect of each frequency can be studied separately.

Simple nonlinear systems may, for small values, be linearized by setting $\sin\varepsilon$ and $\tan\varepsilon$ equal to ε, and setting $\cos\varepsilon \approx 1$.

2.2 Time domain

If the factor $e^{i\omega t}$ cannot be eliminated from each term in the equations, the frequency domain solution does not exist. Examples may be if the solution includes transient effects in time, if terms in the response oscillate with a different frequency than the input or if the response is otherwise nonlinear in nature.

In such cases, the solution must be realized in time. This means that the equations must be solved numerically in a time interval for a specified input frequency. In order to solve the equations over the entire relevant frequency range, one time simulation must be performed for each frequency.

2.3 Transfer function

The transfer function is the ratio of an output amplitude to an input amplitude of a linear, time-invariant dynamic system which oscillates around zero. Since transfer functions apply only for steady-state systems, they are defined entirely in the frequency domain, and the input and output functions are typically Laplace-transforms of the input and output time signals.

In this report, the term is applied somewhat more loosely; on occasion a “transfer function” is defined relating a frequency dependent input and a mean-value output, where the input oscillates and the output does not.

2.4 State space

A linear state space model represents a physical system as a set of linear first order differential equations where the variables are grouped as input, output and internal state variables. For an equation of order n, the state space representation is achieved by transforming the equation into n first order equations with a total of n state variables.

A state space representation of frequency domain equations will yield identical results as the transfer function. However, the state space approach is not limited to the frequency domain: state space models can readily be implemented in time domain models. Implementing certain functions into time domain models may be laborious, and approximating these functions using state space representations may save CPU-time.

3 Theory

3.1 Linear wave-vessel response theory

3.1.1 Wave potential

The material presented here is from (Fathi). Elaborations can also be found in (Faltinsen 1993), (Newman 1978) and (Fossen 2011) or any introductory book on water waves. All symbols are defined in the nomenclature.

Linear water waves can be described by a scalar function from which the velocities and pressure can be determined. In the xz-plane, this *wave potential* has the form:

$$\phi\left(x,z,t\right) = \frac{g\zeta_a}{\omega_0} e^{kz} e^{-ikx} e^{i\omega_0 t} \tag{3.1}$$

Assume a body is traveling with a speed U in the xz-plane defined by ϕ. The encounter potential it experiences is written as

$$\phi_e\left(x,z,t\right) = \frac{g\zeta_a}{\omega_0} e^{kz} e^{-ikx} e^{i\omega_e t} \tag{3.2}$$

where $\omega_e = \omega_0 + \frac{{\omega_0}^2}{g} U$ is the encounter frequency.

The vertical velocity and acceleration of the water particles are given by

$$w = \omega_0 \zeta_a e^{kz} e^{-ikx} e^{i\omega_e t} \tag{3.3}$$

$$\dot{w} = i\omega_e \omega_0 \zeta_a e^{kz} e^{-ikx} e^{i\omega_e t} \tag{3.4}$$

3.1.2 Frequency domain

Assume a wave potential in steady state condition with a vessel floating or moving on the free surface. This implies that the waves and vessel oscillate harmonically with no transient effects present, and that the wave loads on the structure oscillate with the same frequency as the waves. The total wave potential can be described in terms of three potentials that can be superimposed: the incoming wave potential, the diffraction potential that arises du to waves that are reflected off

the vessel surface, and the radiation potential, that describe the waves set up by the motions of the floating vessel. By integrating the pressure terms from each of these potentials, it can be shown that the following second order linear differential equation describes the rigid body motion of the vessel:

$$\left(\mathbf{M}+\mathbf{A}\right)\ddot{\boldsymbol{\eta}}+\mathbf{B}\dot{\boldsymbol{\eta}}+\mathbf{C}\boldsymbol{\eta}=\mathbf{F}_{ex} \tag{3.5}$$

The coefficients A and B are frequency dependent. Equation (3.5) represents the common frequency domain equation governing vessel response theory. Elaborations can be found in (Fossen 2011), (Faltinsen 1993, Faltinsen 2005), (Eitzen 2012) and (Newman 1978).

3.1.3 Time domain

The following is a summary of material from (Fossen 2011), (Perez and Fossen 2009), and (Eitzen 2012), where details of theory and applicability may be found.

When working in the time domain, the equations must be able to take into account transient effects, i.e. impulse responses. Assume that in addition to the wave potentials mentioned above, a fourth impulse potential is introduced, which fulfils the boundary condition on the vessel when it responds to an impulse load. The result is the Cummins equation, which defines the vessel rigid body motion in the time domain.

$$\left(M+A\left(\infty\right)\right)\ddot{\eta}+\int_{-\infty}^{t}K\left(t-\tau\right)\dot{\eta}\left(\tau\right)d\tau+C\eta=F_{ex} \tag{3.6}$$

The convolution integral term appears due to integration of the impulse response. It is often called the *fluid memory* term, and handles the transient dynamics in the system. The factor $K\left(t\right)$ is called the *retardation function,* and is related to the added mass and damping by:

$$K\left(t\right)=-\int_{0}^{\infty}\omega\left[A\left(\omega\right)-A\left(\infty\right)\right]\sin\left(\omega t\right)d\omega \tag{3.7}$$

$$K\left(t\right)=-\int_{0}^{\infty}\left[B\left(\omega\right)-A\left(\infty\right)\right]\cos\left(\omega t\right)d\omega \tag{3.8}$$

Performing continuous numerical time integrations in a time domain model is not efficient, and it is useful to approximate the fluid memory term with a state space model of the form

$$\begin{aligned} \dot{x} &= A_{ss}x + B_{ss}\dot{\eta} \\ \mu &= C_{ss}x \end{aligned} \tag{3.9}$$

where A_{ss}, B_{ss} and B_{ss} are the state-, input- and output matrices, respectively and x the state vector. The vessel velocities, $\dot{\eta}$, are input to the state space model, and μ is an approximation for the fluid memory term.

Methods exist to find or estimate the infinite added mass coefficient $A(\infty)$. (Perez and Fossen 2008, Perez and Fossen 2009).

In this study, the following steps are performed in order to approximate the fluid memory term:

1. $A(\infty)$ is estimated by finding the added mass for a very high frequency using the ShipX VERES software.
2. $K(t)$ is estimated by integrating numerically over a relatively large frequency range.
3. In order to use $K(t)$ in a state-space model it must be ensured that $K(t)$ is numerically stable when realized in time. Therefore, $K(t)$ is approximated using the Matrix Fitting Toolbox for MATLAB (Gustavsen 2009). This produces coefficients to the state space representation in (3.9) which are implemented in SIMULINK.

3.2 Foil theory

3.2.1 Steady foil theory

Consider a foil placed in an infinite domain of ideal fluid with a uniform incoming velocity U. Coordinates are as shown in Figure 1. Linear foil theory requires that the velocity field $|\nabla\varphi|$ set up by the foil has values much smaller than the undisturbed velocity U. For a foil placed in a coordinate system as shown in Figure 1, this means that all values of the foil geometry in z-direction are small compared to the chord and span values. I.e. the maximum thickness of the foil must be much smaller than the chord length: typically, t/c = 0.06-0.12 for hydrofoils and propeller blades (Minsaas and Steen 2008). It also means that the angle of attack and max camber must be small. See Figure 2 for definitions.

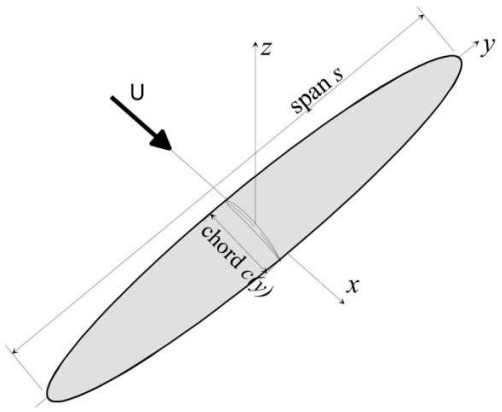

Figure 1: Coordinate system and foil geometry definitions.

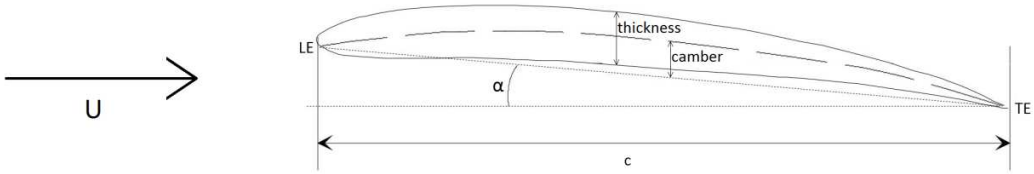

Figure 2: 2D foil geometry definitions (Steen 2010)

When deriving linear foil theory one starts with linearizing the body boundary condition. This is done by assuming that the outward normal vector on the foil surface has a horizontal component which is much smaller than its vertical component, i.e. $n_1 << n_2$ in Figure 3 (note the different axes definitions compared to Figure 1).

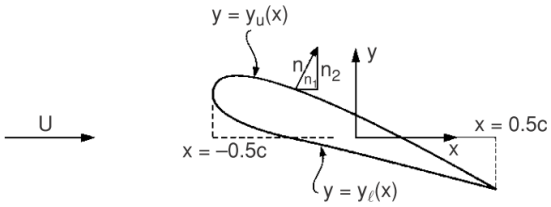

Figure 3: Linearization of a 2D steady flow infinite fluid boundary value problem (Faltinsen 2005)

In a realistic flow around a foil one can observe that the flow leaves the trailing edge tangentially. This phenomena is called the Kutta condition, and is accounted for in the ideal flow situation by superimposing a circulation in the flow field surrounding the foil. This circulation defines the difference in velocities at the upper and lower sides of the foil, giving rise to pressure differences between the two sides. The resultant pressure force is given by the Kutta-Joukowski formula:

$$F = -\rho U \Gamma \left[N/m \right] \tag{3.10}$$

It can be shown that this force is directed perpendicular to the incoming flow direction (Kroo 2007). The lift and drag forces are defined as the forces perpendicular to and in line with the incoming flow, respectively. As a consequence, the lift and drag will be:

$$\begin{aligned} L &= -\rho U \Gamma \\ D &= 0 \end{aligned} \tag{3.11}$$

Lift

The circulation around a foil is generally distributed over the foil and not located in a single point, so that

$$\Gamma = \int_c \gamma(x) dx \tag{3.12}$$

Disregarding the horizontal normal vector, as discussed, one can therefore model the circulation around the foil as a vortex distribution along a section of the x-axis with length c, as shown in Figure 4.

Figure 4: 2D linearized body boundary condition for a flat plate in steady infinite flow (Faltinsen 2005).

It can be shown that the lift force for a flat plate is proportional to the angle of attack:

$$L = \rho U^2 c \pi \alpha \left[N/m \right] \tag{3.13}$$

The 2D lift coefficient is defined as

$$C_L = \frac{L}{\frac{1}{2}\rho c U^2} = 2\pi\alpha \tag{3.14}$$

Assuming an elliptical foil with high aspect ratio, it can be shown that the 3D lift coefficient becomes

$$\begin{aligned} C_L &= \frac{2\pi\alpha}{1 + \frac{2}{\Lambda}} \\ &= C_{L0} \cdot \alpha \end{aligned} \tag{3.15}$$

where $\Lambda = \frac{s^2}{A}$ is the aspect ratio.

Details regarding linear foil theory can be found in (Faltinsen 2005), and more rigorously in (Kármán and Burgers 1935).

For a 2D foil with a turbulent boundary layer propagating in infinite fluid, linear theory may be valid up to α = 17° (Faltinsen 2005), upon which leading edge separation will occur and the foil will begin to stall.

Drag

In addition to the lift force, two drag components will act on the foil: potential and viscous drag. The first arises due to 3D pressure effects, and the latter is found experimentally and is valid for 2D foils.

Potential drag

Within 2D linear foil theory, there will be no drag on the foil, as seen in equation (3.11). Potential drag (or induced drag) arises due to a spanwise circulation distribution over the foil. For an elliptical foil, it can be shown that the drag can be expressed in terms of the lift as (Faltinsen 2005):

$$C_D = \frac{{C_L}^2}{\pi\Lambda} \tag{3.16}$$

Viscous drag

In order to include viscous foil drag one must assume a foil geometry. For this project, the symmetrical NACA 0012 wing section is applied. The empirical lift-drag curve can be found in (Abbott and Doenhoff 1959) and it is also given in Appendix 1: NACA 0012.

Comment on 3D foil theory

It has already been mentioned that the foil is assumed to be elliptical. The sectional forces along the span of the foil will thus vary with the sectional chord length. Instead of integrating the forces along the span, it is assumed that the mean chord length is a valid measure in the calculations of the 3D lift and drag. The mean chord length is related to the max chord by:

$$c_{mean} = c = \frac{1}{4}\pi c_0 \tag{3.17}$$

A lower case *c* without any subscript will from now on denote the mean chord length unless specifically defined otherwise.

Due to the continuous trailing vortices shed along the span, the sectional angle of attack will vary along the span. For an elliptical foil, the circulation can be integrated along the span to give the closed-form expressions in equations (3.15) and (3.16).

The reader is referred to (Kármán and Burgers 1935, Abbott and Doenhoff 1959, Faltinsen 2005, Minsaas and Steen 2008, Steen 2010) amongst others for more elaborate discussions on linear foil theory.

3.2.2 Unsteady foil theory

In this chapter is presented a conceptual introduction to unsteady foil theory. More rigid mathematical derivations of the equations governing unsteady foil theory can be found in (Breslin and Andersen 1996), (Kroo 2007), (Newman 1978), (Sears 1941), (Theodorsen 1934) and (Dimitriadis). Arguments, assumptions and relations that are not referenced are the author's own contribution.

Motivation

For a foil in a flow with a sinusoidally oscillating angle of attack, the forces on the foil will oscillate accordingly. To understand why this is interesting from a propulsion point of view, consider the foil in Figure 5. It is moving with a constant horizontal velocity U while oscillating in heave with velocity $\dot{z}$. The instantaneous angle of attack is

$$\alpha = \arctan\left(\frac{-\dot{z}}{U}\right) \approx \frac{-\dot{z}}{U} \tag{3.18}$$

for small α . The lift force L is oriented perpendicular to the instantaneous inflow direction, thus oscillating between an inclined upwards direction and an inclined downwards direction. The horizontal component of the lift force will always be directed parallel to the foil propagation direction and will oscillate around a negative value (ref. the coordinate system in Figure 1), i.e. resulting in a mean thrust force acting in the opposite direction of the incoming flow. This thesis in concerned with exploring the thrust possibilities of an oscillating foil on a vessel.

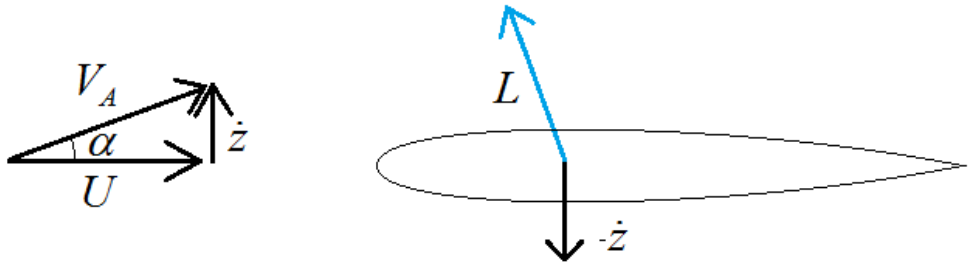

Figure 5: 2D foil oscillating in heave

In the following subchapters, the forces acting on an oscillating foil will be discussed.

Angle of attack

Consider Figure 6. A foil moves with a constant velocity U in a flow field while oscillating with frequency ω in heave, h , and pitch, δ. The flow field also has oscillating vertical components:

$$\begin{aligned} h &= h_0 e^{i\omega t} \\ \delta &= \delta_0 e^{i\omega t} \\ w &= w_0 e^{i\omega t} \end{aligned} \tag{3.19}$$

The linearized vertical velocity of the foil can be expressed as (Eitzen 2012):

$$\begin{aligned} v_{rel} &= w - \dot{h} - U\delta \\ &= \dot{z} - U\delta \end{aligned} \tag{3.20}$$

where $\dot{z}$ is the contribution that is vertical according to the coordinate system and $U\delta$ corrects for the foil pitch angle. The velocities w and $\dot{h}$ are oppositely directed, hence the minus sign. The foil will "feel" the effective inflow, V_A, at an angle

$$\varphi = \arctan\left(\frac{\dot{z}}{U}\right) \tag{3.21}$$

The effective angle of attack, α_e, is defined as

$$\alpha_e = \varphi - \delta \tag{3.22}$$

$$= \arctan\left(\frac{\dot{z}}{U}\right) - \delta \tag{3.23}$$

$$\approx \frac{\dot{z}}{U} - \delta \tag{3.24}$$

Note that even though α_e and δ depend on each other, both are independent of φ, which is given only by the vertical oscillation and the flow. Thus, when the vertical velocities are known, this opens up for controlling the effective angle of attack by controlling the phase and magnitude of the pitch angle.

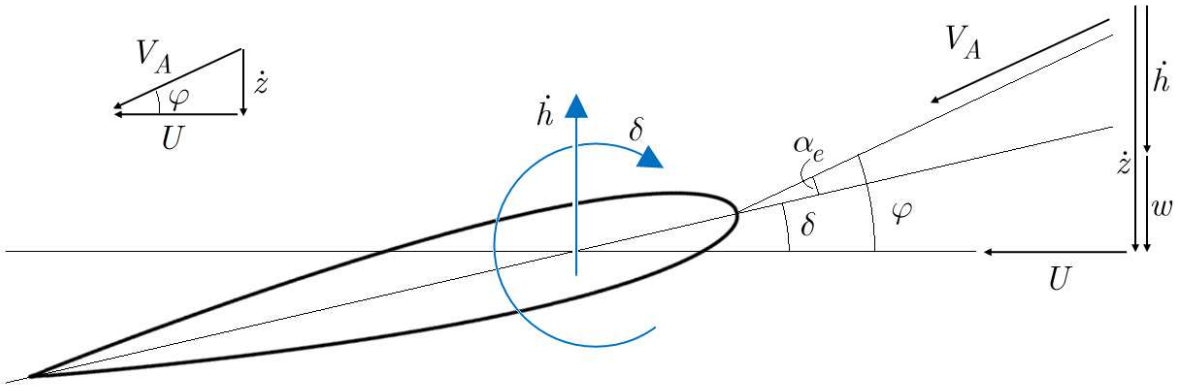

Figure 6: Definition of angles and velocities.

Circulatory force - lift

The ideal flow situation on which linear foil theory is based implies that the fluid is irrotational and inviscid. Hence, no shear stresses arise between water particles, and the rotation rate of the fluid particles cannot change in time. Therefore, any circulatory fluid motion about any closed

contour moving with the fluid domain will remain constant. This is called Kelvin's theorem of the conservation of circulation (Dimitriadis)

When the foil or incident flow are perturbed so that the forces on the foil change, a change in the flow field surrounding the foil will also occur. This implies that the circulation around the foil changes. In order to comply with Kelvin's theorem, a vortex is therefore immediately shed from the trailing edge into the wake and convected downstream. The vortex is oppositely directed to the change in circulation experienced during the perturbation.

Thus, for a 2D foil experiencing a continuous oscillating flow situation, a continuous vortex street will be shed into the wake. This vortex street will induce velocities in the fluid domain, and thus influence the velocities in front of the foil, and therefore also the instantaneous angle of attack. Since the magnitude of the shed vortices depend on the magnitude of the perturbations the foil experience, the time history of the foil oscillation will influence the instantaneous angle of attack, and thus the magnitude and direction of the lift. For any given angle of attack, the unsteady effects will reduce the lift compared to the static lift.

For harmonically oscillating flow situation, the time history can be taken care of in a frequency domain analysis. Two analytical approaches and one empirical approach that can be used to correct for the dynamic effects are presented here. The analytical approaches assume a 2D steady-state oscillatory system, while the empirical approach is valid for finite aspect ratio foils.

Theodorsen approach

Consider a 2D foil oscillating in heave and pitch in a uniform flow. The lift is given as:

$$L^{2D} = \frac{1}{2}\rho c U^2 C_L C(k_f) \left[N/m \right] \tag{3.25}$$

where $k_f = \frac{\omega c}{2U}$ is the *reduced frequency*. Equation (3.25) is similar to the expression used in linear foil theory, apart from the presence of the correction factor, $C\left(k_f\right)$. This correctino factor is called the Theodorsen function (Newman 1978, Faltinsen 2005), and is defined by the Hankel functions:

$$C(k_f) = F(k_f) + iG(k_f) = \frac{{H_1}^{(2)}(k_f)}{{H_1}^{(2)}(k_f) + i{H_0}^{(2)}(k_f)} \tag{3.26}$$

Note that $C\left(k_f\right)$ will have a complex value. This means that the oscillatory motion not only affects the magnitude of the force, but also the phase angle between the angle of attack and the lift. Thus, the Theodorsen function introduces a time lag in the lift term in equation (3.25), which means that the lift will not necessarily be at its max when the angle is at its max. Also the imaginary term is frequency dependent, which means that the resulting time lag will vary with oscillation frequency.

The definition of lift coefficient, which can be found in (Faltinsen 2005) or any introduction to linear foil theory, is:

$$C_L = \frac{L^{2D}}{\frac{1}{2}\rho c U^2} \tag{3.27}$$

Compare equations (3.25) and (3.27) to get:

$$C_L C\left(k_f\right) = \frac{L^{2D}}{\frac{1}{2}\rho c U^2} = C_{Lu} \tag{3.28}$$

Here, the unsteady lift coefficient, C_{Lu}, is introduced. The definition of unsteady lift in (3.25) gives the impression that the lift force and not the lift coefficient is corrected for. However, the Theodorsen function includes the unsteady wake to correct for the velocities in front of the foil, thus correcting the angle of attack.

The lift coefficient C_L is identical to the one given for an elliptical foil in equation (3.15) where for α is used the effective angle of attack given in equation (3.22). Hence,

$$C_L = \frac{2\pi}{1 + 2/\Lambda}\left(\arctan\left(\frac{\dot{h}}{U}\right) - \delta\right) \tag{3.29}$$

and the linearized version:

$$C_L = \frac{2\pi}{1 + 2/\Lambda}\left(\frac{\dot{h}}{U} - \delta\right) \tag{3.30}$$

The unsteady lift coefficient becomes:

$$C_{Lu} = \frac{2\pi}{1 + \frac{2}{\Lambda}} C\left(k_f\right)\left(\arctan\left(\frac{\dot{h}}{U}\right) - \delta\right) \tag{3.31}$$

and the linearized version:

$$C_{Lu} = \frac{2\pi}{1 + \frac{2}{\Lambda}} C\left(k_f\right)\left(\frac{\dot{h}}{U} - \delta\right) \tag{3.32}$$

$$= C_{L0} C\left(k_f\right) \alpha_{e0} \cdot e^{i\omega t} \tag{3.33}$$

A comment must also be made regarding the velocity in equation (3.25). For larger angles, the instantaneous inflow velocity will be $V_A = \frac{U}{\cos\varphi}$. In the derivation of the Theodorsen function, infinitely small disturbances are assumed. (Theodorsen 1934). However, (Leishman 2006) states that the Theodorsen function is suitable for flow oscillation amplitudes of up to 70% of the uniform incoming flow. Inspired by this, the following modification is applied to the lift:

$$L^{2D} = \frac{1}{2}\rho c \frac{U^2}{\cos^2\varphi} C_L C(k_f) \tag{3.34}$$

Sears approach

Sears' approach is slightly different than that of Theodorsen. Here, the foil is held steady in a flow field with oscillating vertical velocity components. The angle of attack is now given by the vertical velocity of the water particles, w :

$$\begin{aligned} \alpha_e &= \arctan\left(\frac{w}{U}\right) - \delta \\ &\approx \frac{w}{U} - \delta \end{aligned} \tag{3.35}$$

In this case, the dynamic effects are accounted for with the Sears function (Newman 1978):

$$Se(k_f) = \frac{2i/\pi k_f}{H_1^{(2)}(k_f) + iH_0^{(2)}(k_f)} \tag{3.36}$$

which will correct for the lift in the same way as the Theodorsen function in equation (3.34).

Empirical approach

The two previous approaches are only valid for 2D unsteady theory. (Minsaas and Steen 2008) presents an empirical formula originally introduced by (Breslin and Andersen 1996) which relates the quasi static lift to the unsteady lift for a finite aspect ratio foil in the following manner:

$$\frac{C_{Lu}}{C_{Lqs}} = 1 - \left(\frac{k_f}{3}\right)^{0.35} \cdot \left[1 - 0.88 \cdot \left(\frac{\Lambda}{6}\right)^{0.21}\right] \cdot \Lambda \tag{3.37}$$

The advantage of the empirical approach is that, since found empirically, it is assumed valid for finite aspect ratio foils. It does, however, not include any information about the phase shift of the unsteady lift, and thus gives an unsteady lift which will be in phase with the quasi-static angle of attack.

For simplicity, only the Theodorsen is used in the model calculations in this study.

Drag

The relations between lift and drag presented in *3.2.1 Steady foil theory* are assumed valid also for unsteady theory. Since linear foil theory applies for stationary flow, it only relates the force magnitudes. When extending the theory to include time dependence, assumptions must therefore be made regarding how the forces are related in time. Hence, it is simply assumed that the drag forces are in phase with the lift. The consequences will be elaborated on in the following.

Potential drag

Introduce the unsteady lift from equation (3.33) into the lift-drag relation given in equation (3.16) yields:

$$C_{Dp} = \frac{{C_{Lu}}^2}{\pi\Lambda} = \frac{{C_{L0}}^2 C^2 {\alpha_{e0}}^2}{\pi\Lambda} e^{i2wt} \tag{3.38}$$

where $C\left(k_f\right)$ is shortened to C for readability.

Note that the potential drag will oscillate with the double frequency of the foil oscillation.

The unsteady drag will also be influenced by the Theodorsen correction. Recall that the Theodorsen function corrects not only the magnitude, but also the phase of the lift. Thus, since the unsteady lift is proportional to $C\left(k_f\right)$, and the unsteady drag is proportional to $C\left(k_f\right)^2$,

the drag will not be in phase with the lift, violating the assumption stated above. This is amended by the following arguments:

Recall that the Theodorsen function is only applicable for 2D foils, while the potential lift-drag relation is given for a 3D steady foil where time lag is not an issue. I.e. introducing the Theodorsen function in the drag definition in (3.38) is simply a result of the engineering approach combining 2D and 3D foil theory, and is not meaningful with regard to the phase. It is therefore simply assumed that the drag is in phase with the lift, as this will fulfill the lift-drag relation at all points in time. Note that since the drag oscillates with double the frequency of the lift, the phrase "in phase with" here is defined to mean that the drag maxima are in phase with the lift extrema.

The unsteady drag is thus modified to:

$$C_{Dp} = \frac{{C_{L0}}^2}{\pi\Lambda} C \cdot \left|C\right| \cdot {\alpha_{e0}}^2 \cdot e^{i2wt} \tag{3.39}$$

where the $\left|\ \right|$ represent the absolute value. Using this expression, the assumption that the drag and lift are in phase is fulfilled, while the Theodorsen function squared is present in compliance with equation (3.28).

Viscous drag

Assuming the viscous drag to be proportional to ${C_L}^2$, the viscous drag will also oscillate with frequency 2ω. The viscous lift-drag curve for the NACA 0012 profile with a smooth surface and Reynolds number $9 \cdot 10^6$ is interpolated using a second order polynomial. This is shown in Figure 7. Because it is empirical, the original lift-drag curve is not entirely symmetric about $C_L = 0$. In order to create a consistent model, however, the lift-drag relation must be equal for positive and negative angles of attack. Therefore, only values from the right half-plane have been extracted. These were mirrored about $C_L = 0$ to create the symmetric polynomial shown in Figure 7.

The interpolated polynomial has the form:

$$C_{Dv} = A_2 \cdot {C_L}^2 + A_0 \tag{3.40}$$

where

$$A_0 = 5.5927e\text{-}3$$
$$A_2 = 4.1176e\text{-}3$$

The viscous drag will also be influenced by the Theodorsen function. This may seem counterintuitive since the Theodorsen function is connected to pressure forces in an inviscid flow, and within linear theory viscous and pressure forces are treated as two separate phenomena and superimposed. However, there is a physical relation between the velocity over the foil and the viscous drag. This can be modelled empirically as a relation between the lift and the viscous drag, as in (Abbott and Doenhoff 1959). Hence, since the Theodorsen function represents the physical reduction in lift, and assuming that also the viscous drag is in phase with the lift, the same proportionality applies for C_{Dv} as for C_{Dp}:

$$C_{Dv} = A_2 \cdot {C_{L0}}^2 \cdot C \cdot \left|C\right| \cdot {\alpha_{e0}}^2 \cdot e^{i2wt} + A_0 \tag{3.41}$$

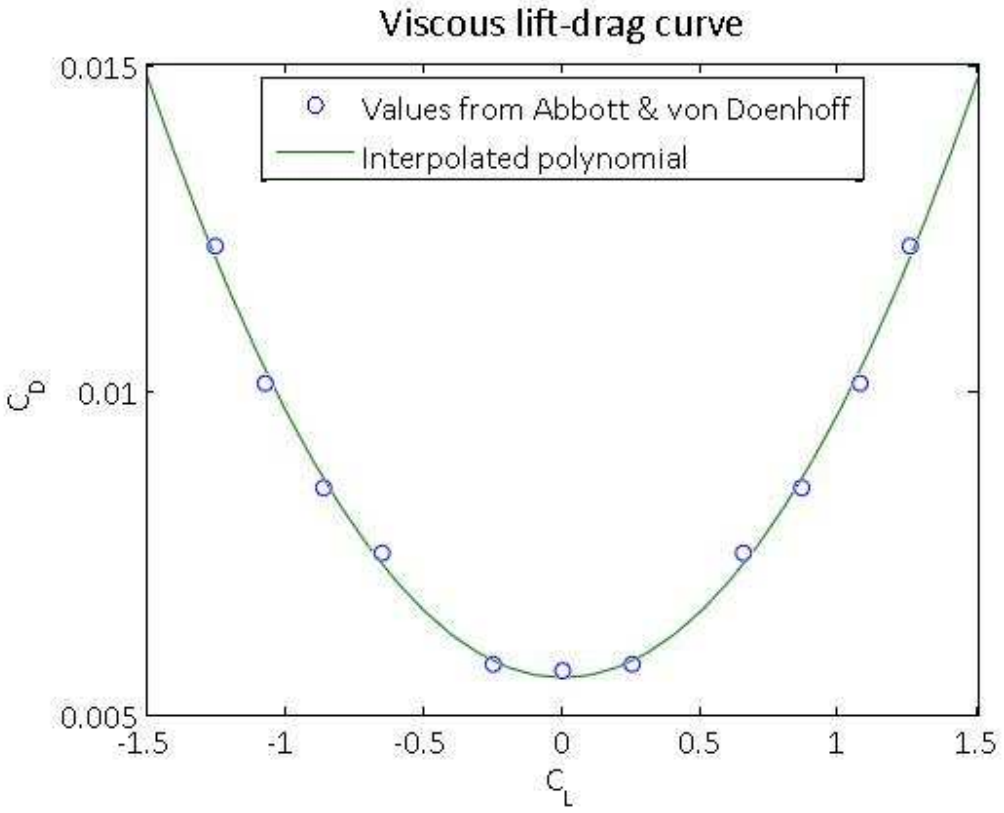

Figure 7: Viscous drag. The blue circles represent values as given in the right-half of the original in Abbott & von Doenhoff. The green line shows the interpolated curve.

Added mass

It can be shown that the 2D added mass coefficient for a flat plate oscillating in heave is:

$$a_{33F} = \frac{1}{4}\rho\pi {c_{proj}}^2 \tag{3.42}$$

where c_{proj} is the length of the 2D plate projected on to the horizontal plane. For a foil oscillating in both heave and pitch, the projected chord length will be $c_{proj} = c\cos\delta$, which will be time dependent and may be significantly less than c for large pitch angles. This is however neglected, and for simplicity it is assumed that $c_{proj} = c$ throughout the study. Also, the foil added moment is neglected.

The added mass in heave is purely vertical. It is proportional to the vertical acceleration of the foil and will oscillate with the same frequency as the foil:

$$F_{3Add} = a_{33F}\ddot{z} \tag{3.43}$$

This is the same definition that is used by (Eitzen 2012). The non-dimensionalized added mass coefficient of the foil is defined as

$$C_{addF} = \frac{F_{3Add}}{\frac{1}{2}\rho c U^2} = \frac{a_{33F}\left(\dot{w} - \ddot{h}\right)}{\frac{1}{2}\rho c U^2} \tag{3.44}$$

The added mass is linear and will oscillate with the same frequency as the foil oscillation.

Damping

Within potential theory, damping forces are proportional to velocity terms and represent energy that is carried away from the system through radiating waves. A foil operating close to the free surface will be likely to set up radiating waves, and these waves will induce velocities that will change the angle of attack. Due to lack of a damping model for a foil or a flat plate close to the free surface, the damping forces have been neglected from the project.

The consequences of this assumption are unknown. The assumption does, however, come with one fine advantage:If a damping term is to be included, it will be likely to introduce a fluid memory effect in a time domain model. This is now avoided.

Note that regardless of this assumption, additional damping forces will appear when the foil is connected to a vessel. This will introduce fluid memory terms in the combined vessel-foil model that must be approximated in the time domain.

Advance

The *advance force,* A_F, is here defined as the component of the lift force projected on to the horizontal plane. The terms “advance force” and “advance coefficient” in this project must not be mistaken for the same terms commonly used in propeller theory.

It is displayed in green in Figure 8, and is defined in the following way:

$$\begin{aligned} A_F &= L\sin\varphi \\ &= \frac{1}{2}\rho c\frac{U^2}{\cos^2\varphi}C\cdot C_{L0}\cdot\alpha_e\sin\varphi \\ &= \frac{1}{2}\rho c U^2 C\cdot C_{L0}\cdot\frac{\tan\varphi}{\cos\varphi}\alpha_e \end{aligned} \tag{3.45}$$

which leads to the definition of the advance coefficient

$$C_{adv} = C\cdot C_{L0}\cdot\alpha_e\cdot\frac{\tan\varphi}{\cos\varphi} \tag{3.46}$$

The linear advance coefficient is:

$$C_{adv} = C\cdot C_{L0}\cdot\alpha_e\cdot\varphi \tag{3.47}$$

Consider the linear advance coefficient. Both a_e and φ oscillate with the foil oscillation frequency, and as a consequence, the advance coefficient will oscillate with the double frequency. Also, from Figure 8 and from the definitions of a_e and φ it can be seen that the two angles will always have the same sign. This gives a mathematical reason for calling the force component *advance*: the value may be zero, but it is never negative.

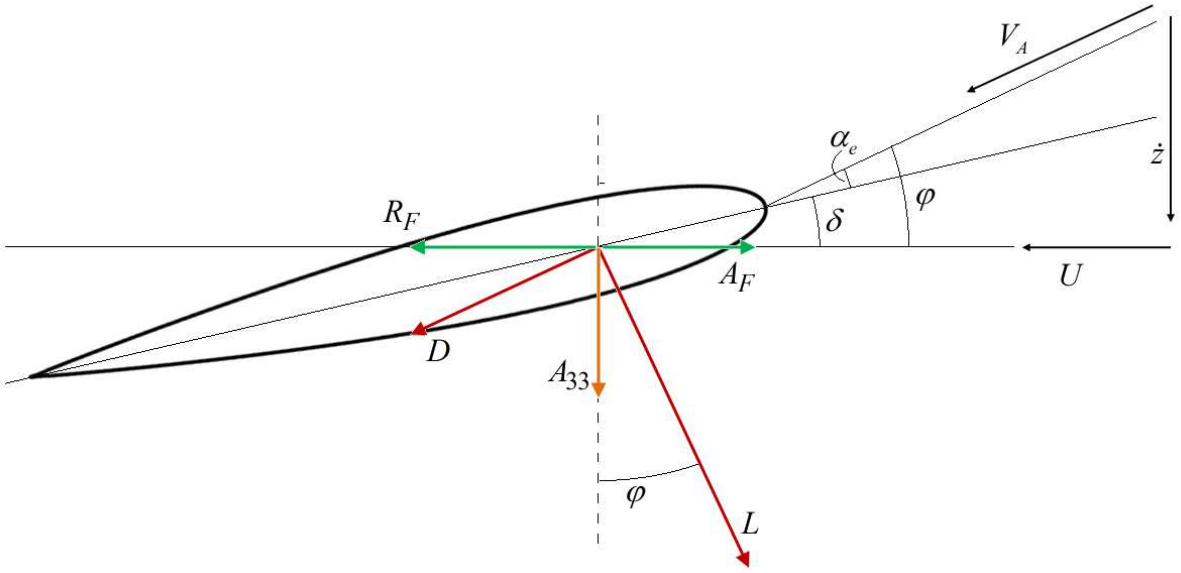

Figure 8: Forces on an oscillating foil. Lift and drag in red. Added mass in orange. Horizontal components in green.

Resistance

The *foil resistance force*, R_F, is here defined as the component of the drag force projected on to the horizontal plane. Both the potential and viscous drag are included. The resistance is displayed in green in Figure 8, and is derived in the following way:

$$\begin{aligned} R_F &= D\cos\varphi \\ &= \frac{1}{2}\rho c\frac{U^2}{\cos^2\varphi}\left[C_{Dp}+C_{Dv}\right]\cdot\cos\varphi \end{aligned} \tag{3.48}$$

$$= \frac{1}{2}\rho c\frac{U^2}{\cos\varphi}\left[C\cdot|C|\cdot {C_{L0}}^2\cdot {\alpha_{e0}}^2 B_2 + A_0\right] \tag{3.49}$$

where $B_2 = \left(\frac{1}{\pi\Lambda}+A_2\right)$. This gives the following definition of the foil resistance coefficient:

$$C_{res} = \left[C\cdot|C|\cdot {C_{L0}}^2\cdot {\alpha_{e0}}^2 B_2 + A_0\right]\frac{1}{\cos\varphi} \tag{3.50}$$

The linear resistance coefficient is

$$C_{res} = \left[C \cdot \left| C \right| \cdot {C_{L0}}^2 \cdot {\alpha_{e0}}^2 B_2 + A_0 \right] \tag{3.51}$$

Due to the second order nature of the drag, the resistance will oscillate with the double frequency of the foil oscillation.

Thrust

The *thrust force* is defined as the difference between the advance and the resistance:

$$T = A_F - R_F \tag{3.52}$$

The thrust coefficient is consequently:

$$\begin{aligned} C_T &= \frac{T}{\frac{1}{2}\rho c U^2} \\ &= C_{adv} - C_{res} \end{aligned} \tag{3.53}$$

$$\begin{aligned} C_T = C \cdot C_{L0} \cdot \alpha_e \cdot \frac{\tan\varphi}{\cos\varphi} \\ - C \cdot \left| C \right| \cdot {C_{L0}}^2 \cdot \frac{{\alpha_{e0}}^2}{\cos\varphi} B_2 - \frac{A_0}{\cos\varphi} \end{aligned} \tag{3.54}$$

The thrust will oscillate with the double frequency of the foil.

The linear thrust is defined as:

$$C_{Tlin} = C \cdot C_{L0} \cdot \alpha_e \cdot \varphi - C \cdot \left| C \right| \cdot {C_{L0}}^2 \cdot {\alpha_{e0}}^2 B_2 - A_0 \tag{3.55}$$

Average thrust

The value of interest in this study is the time-average thrust. Previous master students have derived methods to find the time-average thrust in the frequency domain (Borgen 2010, Eitzen 2012). By integrating the linear equations over one oscillation period, the average thrust could be expressed in terms of closed-form mathematical expressions that were proportional to the wave amplitude. This allowed for all the components in the thrust expression to be defined in terms of RAO's.

The methods of Borgen and Eitzen are elegant. However, they require that both α_e and φ are within the linear limit. As mentioned, this may not be the case, resulting in integrands of the form $\cos\left(\varphi_0 e^{i\omega t}\right)$ and $\cos\left(\varphi_0 e^{i\omega t}\right)$. Neither (Rottmann 2003) nor (Wolfram|Alpha 2013) could

provide closed-form integrals of these terms. Also, in this project, active foil propulsion in calm water is studied, and defining the response in terms of a RAO proportional to the wave amplitude is meaningless.

In this study, a less elegant time averaging is applied. Using MATLAB, the equations are realized in time by inserting $e^{i\omega t}$ in the equations and letting the time run long enough to cover multiple oscillation periods. After the time series are realized, the mean is found numerically.

Vertical forces

The total vertical force on the foil is of interest for the combined foil-vessel model. The effects of viscous drag and added mass will be discussed. Apart from these effects, the derivation proposed here is similar to that of (Borgen 2010).

The vertical force on the foil is:

$$F_V = L\cos\varphi + D\sin\varphi + A_{33F} \tag{3.56}$$

The drag contribution is assumed negligible to the total force. Also, the drag contribution will oscillate with two frequency components and is not possible to include in a frequency domain study. Hence, the expression for the vertical force becomes

$$F_V = \frac{1}{2}\rho c \frac{U^2}{\cos^2\varphi} C \cdot C_{L0} \cdot \alpha_e \cos\varphi + a_{33F}\left(\dot{w} - \ddot{h}\right) \tag{3.57}$$

Both terms oscillate with the oscillation frequency of the foil, and the vertical forces can thus be studied in the frequency domain.On non-dimensional form, the force is:

$$C_V = C \cdot C_{L0} \cdot \frac{\alpha_e}{\cos\varphi} + C_{addF} \tag{3.58}$$

Optimal angle of attack

(Eitzen 2012) includes a short discussion on the optimal angle of attack, and attempts to find an expression that can be applied in the simulations. Inspired by this, a similar approach is discussed here. The approach starts by differentiating the thrust with respect to α_e in order to find the maximum.

$$\frac{\partial C_T}{\partial \alpha_e} = 0$$

$$\Downarrow \tag{3.59}$$

$$0 = -2C \cdot \left|C\right| \cdot {C_{L0}}^2 \cdot \frac{B_2}{\cos\varphi}\alpha_e + C \cdot C_{L0} \cdot \frac{\tan\varphi}{\cos\varphi}$$

$$\Downarrow$$

$$\alpha_{opt} = \frac{\tan\varphi}{2\left|C\right|C_{L0}B_2} \tag{3.60}$$

$$= \frac{\tan\varphi}{2\left|C\right|\frac{2\pi}{1+\frac{2}{\Lambda}}\left(\frac{1}{\pi\Lambda}+A_2\right)}$$

$$= \frac{\Lambda+2}{4\left|C\right|\left(1+\pi\Lambda A_2\right)}\tan\varphi \tag{3.61}$$

Thus, the optimal angle of attack appears to be dependent on the aspect ratio, frequency and the angle of the instantaneous inflow velocity.

Without the viscous drag contribution, A_2, the denominator in equation (3.61) would approach zero for increasing aspect ratio. This means that as the span increases and the 3D effects should decrease, the angle of attack will increase without bounds. This has no physical meaning.

The viscous drag term ensures that the value of the angle of attack converges towards a finite value. However, for the lowest frequency in this study, and for $\varphi = 15^\circ$, α_{opt} will approach $5.8\left[rad\right]$ as Λ approaches infinity. Again, this clearly has no meaning.

Why does this approach not work, even for small angles? It is not the unsteady effects that cause the error: the only elements of the equations that arise due to unsteady effects are the Theodorsen factors in C_T. These may be removed from the first and second terms so that the equation describes a stationary flow situation, and the relation will still be valid. φ and α_{opt} are in this equation only amplitude values, and do not oscillate.

The reason for why maximizing the thrust in this way does not work is found in the assumptions and limitations of linear theory, which state:

1. The lift is proportional to the angle of attack. (Faltinsen 2005)
2. Linear theory assumes that all geometric lengths in vertical direction are much smaller than the lengths in the horizontal plane, but there are no limitations inherent in linear foil theory that defines what occurs when the upper limit for the angle of attack is reached. (Faltinsen 2005). This value, the stall angle, must be determined using rules of thumb or stall angles from tabulated foil section profiles.
3. The potential drag is a 3D inviscid effect which will approach zero for increasing aspect ratios. This is consistent with 2D foil theory. (Faltinsen 2005)

Thus, the optimal angle of attack will simply be the largest angle possible. Also, increasing the span or reducing the chord length will reduce the induced drag and contribute to increased thrust coefficient. Recall, however, that the chord length not only appears in the definition of the aspect ratio, but also in the definition of thrust: $T = \frac{1}{2}\rho c U^2 C_T$. Thus for a given span an optimal chord length is likely to exist.

Assume for the moment that there existed a physical phenomenon that could be explained perfectly with linear, inviscid foil theory. The lift and drag coefficients for an elliptical foil are closed-form expressions and would then be true. Would there then exist an angle for which the difference between the drag contribution and the lift contribution is largest? Assuming there is, this angle would be given by the equation

$$\alpha_{opt} = \frac{\Lambda + 2}{4} \tan\varphi \tag{3.62}$$

Which is equation (3.61) for a stationary nonviscous flow. Within the mathematical space defined by this equation, a solution exists. Within the linear model, however, the result is meaningless because it by far exceeds all limitations defined by the linearity assumptions.

As mentioned, the viscous drag contribution brings the result closer to reality because reduces the optimal angle from infinity to a finite value. For large aspect ratio, the angle will approach the 2D value, which in this case is not zero. However, the model still does not give any meaningful results.

Linear foil theory has proven to be applicable to a certain degree also outside the strict limits defined in the assumptions (Faltinsen 2005), (Breslin and Andersen 1996), (Jones and Platzer

1999). The reason that including the viscous term does not fix the problem may be that also the viscous term depends on the lift coefficient. However, unless there is an error that has slipped the author's attention, this discussion suggests that main source of error is connected with reducing the order of the model during the differentiation. This will reduce, or perhaps remove, any meaningful use of the model.

An amendment for this order reduction error could perhaps be abated by representing the linear relation between C_L and α as a Fourier series of, say, 4th order, or any order necessary. Both the lift and drag terms could then be modeled as a finite sum of sine terms, and if enough terms are included the model could be valid also after differentiation. Whether this will actually solve the issue within the limitations of linearity remains unanswered at this point.

In terms of relevance for this study, the preceding discussion has clarified two aspects:

1. The optimal angle of attack will be the largest angle possible for the NACA 0012 wing profile in stationary flow, which is $15°$.
2. Linear theory is an established discipline with distinct relevance, but attempts to extend the theory to other applications must be evaluated carefully even when the equations appear to be mathematically consistent.

Combining 2D unsteady theory with 3D theory

(Kroo 2007) and (Breslin and Andersen 1996) discuss the dynamics that arise when expanding from 2D unsteady theory to 3D unsteady theory. The wake contains trailing vortices distributed along the span in addition to the unsteady wake. The mathematical formulations that arise are "highly resistant to analytical procedures and we must resort to numerical methods." (Breslin and Andersen 1996).

Numerical methods are not considered in this study. The procedures to expand from 2D to 3D theory are presented in the preceding chapter, and amounts to assuming that the relations applicable for elliptical planforms in 3D steady theory also apply for 3D unsteady theory. This assumption is also the foundation of (parts of the) theory described in (Eitzen 2012) and (Fathi).

4 Model simulations and results

The aim of this section is to:

- Apply the theory presented in the previous chapter to specific case studies which may be relevant for marine propulsion
- Study which oscillation frequencies and amplitudes are relevant for propulsion of the vessel presented in this report.
- Show that combining the foil and vessel models is not trivial.

4.1 Foil model

4.1.1 Clarification on equations

A note regarding the boundary condition

Consider equation (3.20), reproduced here:

$$\dot{z} = \dot{h} - U\delta \tag{3.20}$$

According to the arguments presented in chapter 3.2.2 Unsteady foil theory, this equation is important for deriving the relations between the velocities and angles of the foil. However, $\dot{z}$ shoud strictly speaking not represent the relative vertical velocity of the foil, but the linearized body boundary condition on the foil (Faltinsen 2005). The equation will then have the form

$$\dot{z} = \dot{h} - \dot{\delta}x_{rot} - U\delta, \qquad -{}^{c}\!/_{2} < x_{rot} < {}^{c}\!/_{2} \tag{4.1}$$

where x_{rot} is the point of rotation of the foil. I.e. the rotational velocity of the foil will also contribute to the local relative vertical velocity over the foil. This will affect the definition of the effective angle of attack:

$$\alpha_e = \varphi - \delta \tag{3.22}$$

Applying equation (4.1) instead of (3.20), the angle of attack becomes

$$\alpha_e = \varphi - \delta - \frac{\dot{\delta}}{U}x_{rot}$$

Letting $\delta = \delta_0 e^{i\omega t}$ and $x_{rot} = \frac{c}{2}$, the result becomes (after removing the $e^{i\omega t}$ -terms):

$$\alpha_e = \varphi - \delta\left(1 - \frac{\omega c}{2U}\right) \tag{4.2}$$

The second term in brackets can be recognized as the reduced frequency. The range of reduced frequencies present in this report span approximately from 0.06 to 0.8, indicating that the angular velocity term in (4.1) may indeed be significant.

The whole issue can be neglected in the stand-alone foil model by assuming that the foil rotates about mid-chord. However, when connecting the foil to the vessel, this will most likely not be the case in a realistic model. The resultant forces (lift and added mass) are located closer to the leading edge and it makes more sense to locate the rotational point where the moments will be smallest.

Nonetheless, the effect of $\dot{\delta} x_{rot}$ has been neglected in both models: For the foil model, two of three terms in equation (3.22) will be known or defined at all times so that the desired angle of attack can be found for any given δ regardless of the term in the brackets. For the combined foil-vessel model, the ship pitch velocity is assumed to contribute much more to $\dot{z}$ than the foil pitch, $\dot{\delta}$.

Efficiency

Chopra (1976) defines efficiency as the "ratio of the mean rate at which useful work is done to the overall mean rate of working." The definition of "useful work" is not very difficult to work out: the average thrust multiplied by the uniform velocity will provide a sufficient definition. This definition appears also in (Anderson, Streitlien et al. 1998), (DeLaurier 1993) and (Guglielmini and Blondeaux 2004)

The "mean rate of working" is not as trivial to define, however. Chopra (1976) states that the kinetic energy dissipated in the wake must be included. This has also been attempted by Garrick (1936), who found that theoretical efficiencies above 50% only occur for foils that rotate about an axis infinitely far away. Scherer (1968) comments that Garrick (1936) has not included induced velocities in the streamwise direction, thus yielding "an optimistic propulsive efficiency since the kinetic energy lost in the slipstream has not been accounted for."

Nonetheless, Anderson, Streitlien et al. (1998) showed experimentally that "efficiencies higher than 85% can be stably achieved."

In this thesis, the definition of efficieny applied is simple:

$$\sigma = \frac{\overline{C_T U}}{\overline{C_{Lu}\dot{h}} + \overline{C_{addF}\ddot{h}}} \tag{4.3}$$

where the numerator is the mean work necessary to move at forward speed *U*, and the denominator is the mean power necessary to cause the foil to heave. By this definition, a passive foil in an oscillating flow field will have infinite efficiency, since both $\dot{h}$ and $\ddot{h}$ will be zero. This is not realistic because even though δ is constrained to be zero, time-varying moments will affect the foil which will require rotational power to conteract. The definition applied here will therefore overpredict the efficiency.

The kinetic energy dissipated into the wake is not considered, and neither are any vertical viscous effects.

Other definitions mentioned in this theory are the linearized efficiency and the "advance efficiency." The former is simply applies the linearized thrust coefficient from (3.55) while the latter neglects the effect of drag in the numerator:

$$\sigma_{lin} = \frac{\overline{C_{Tlin} U}}{\overline{C_{Lu}\dot{h}} + \overline{C_{addF}\ddot{h}}} \tag{4.4}$$

$$\sigma_{adv} = \frac{\overline{C_{adv} U}}{\overline{C_{Lu}\dot{h}} + \overline{C_{addF}\ddot{h}}} \tag{4.5}$$

4.1.2 Case study

Modeling of an unsteady foil may take many forms, because there are many variables influencing the result. Four simple cases will be studied. The following data are common for all cases:

c_{mean}	3	$[m]$
s	21	$[m]$
z_f	-4	$[m]$
Section profile	NACA 0012	
A	63	$[m^2]$
Λ	7	$[-]$
C_{L0}	4.8869	$[-]$
ρ	1025	$[kg/m^3]$
U	10	$[kn]$

Table 3: Foil and fluid characteristics

The foil is located $4[m]$ below the free surface. The largest oscillation amplitudes studied here are $2.5[m]$. This gives $1.5[m]$ difference between the highest position of the foil and the free surface.

For all cases except Case 1 the stalling limit has been set to $15°$ $(= \pi/12[rad])$.

Case 1: Passive foil in waves

A foil moves with constant horizontal velocity in incoming waves. The foil does not oscillate in neither heave nor pitch. Wave amplitudes from 0.5 to $2.5[m]$ are considered.

The angle of attack for each amplitude is presented in Figure 9. No upper limit has been set for the angle of attack, which reaches a maximum of $18°$. It appears that wave amplitudes above approximately $2.1[m]$ will result in $\alpha_e > 15°$.

The definition of the angle of attack is given in (3.35) and reproduced here for $\delta = 0$:

$$\alpha_e = \arctan\left(\frac{w}{U}\right) \tag{4.6}$$

$$\alpha_e \approx \frac{w}{U} \tag{4.7}$$

The linearized definition will overpredict the angle of attack. However, the difference between the nonlinear (4.6) and linear (4.7) angle of attack is not very significant.

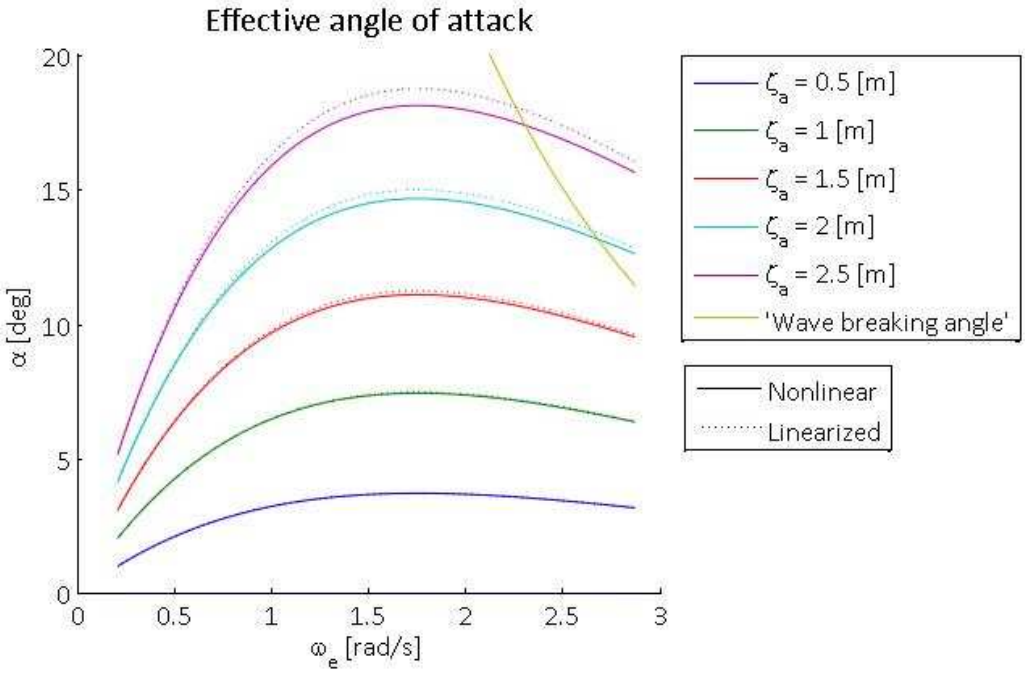

Figure 9: Nonlinear and linear angle of attack for a foil moving in waves with constant velocity.

The reason that the angle of attack first increases with increasing frequency, and then decreases after reaching a max, is found when examining the expression for the angle of attack:

$$\begin{aligned} \alpha_e &\approx \frac{w}{U} \\ &= \frac{1}{U}\left(\omega\zeta_a e^{kz_f} e^{-ikx_f}\right) \end{aligned} \tag{4.8}$$

where $k = \frac{2\pi}{\lambda}$ is the wave number, which increases with frequency. As a rule of thumb, a wave influences the water particle motion approximately half the wavelength below the surface. Thus for increasing wave number, the depth of the wave influence will decrease. This is represented in the e^{kz_f} -factor, which will decrease with increasing frequency (z_f is negative). Since the foil is located at $z_f = -4\left[m\right]$, the wave amplitude at that depth will decrease for increasing frequencies.

In Figure 9 is also shown what is here termed the "wave breaking angle." This takes into account the wave breaking limit from wave theory which states that $H/\lambda = 1/7$ (Faltinsen 2005) where H is the double wave amplitude. From this relation is derived the maximum angle of attack that is possible before the wave will break: the wave breaking angle. Values above and to the right of this curve in Figure 9 will not exist. The derivation is as follows:

$$\omega^2 = kg = \frac{2\pi}{\lambda} g \quad \Rightarrow \quad \lambda = \frac{2\pi}{\omega^2} g \tag{4.9}$$

Equation (4.9) inserted in the wave breaking limit gives

$$2\zeta_a/\lambda \leq 1/7$$
$$\Downarrow$$
$$\zeta_a \leq \frac{\pi g}{7\omega^2} = \zeta_{\max}$$

which, inserted into the expression for the angle of attack, gives

$$\alpha_{\max} = \frac{w}{U} = \frac{\pi g}{7\omega U} e^{kz_f} e^{-ikx_f} \cdot \frac{180}{\pi} \tag{4.10}$$

The last factor $\frac{180}{\pi}$ is inserted to convert from radians to degrees.

Figure 10 shows how the lift coefficient will vary with increasing frequency. The blue line shows the linear quasi-static lift given in equation (3.30), while the turquoise, green and red show the three unsteady correction approaches presented in Chapter 3.2.2. The magenta line shows the

added mass term, which approaches the Theodorsen function for $\omega_e \approx 3\left[rad/s\right]$. The added mass increases for increasing frequency over the entire frequency range shown.

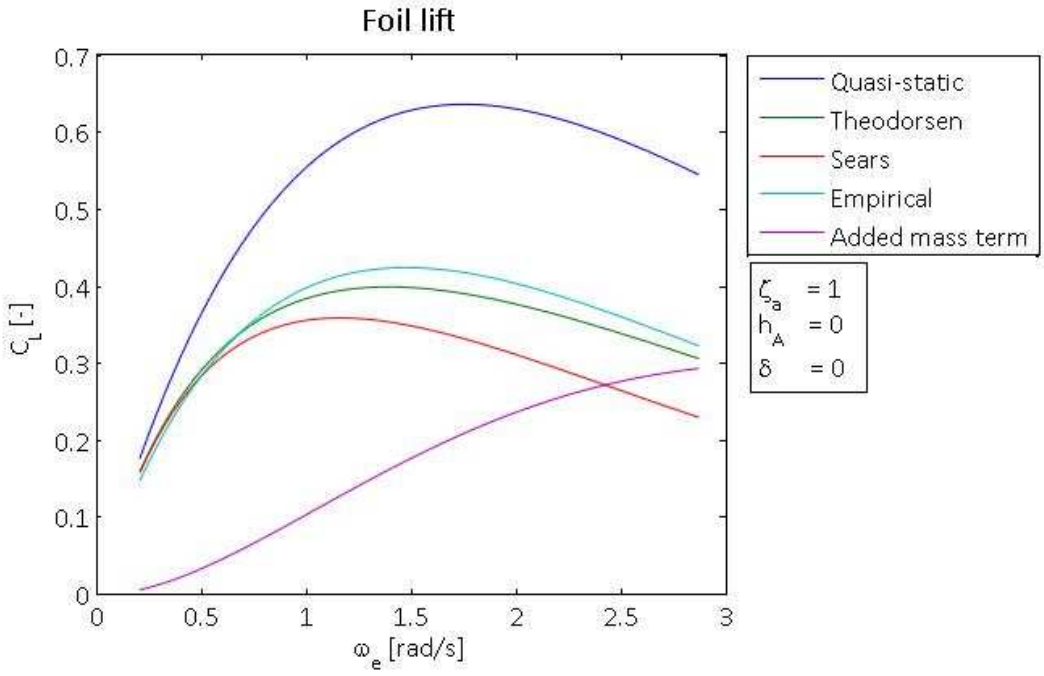

Figure 10: Case 1 - Steady and unsteady lift forces on passive foil in waves of height 1m. The added mass force has been included in magenta.

Figure 11 shows the effect of amplitude and frequency on the vertical force acting on the foil. The difference between linear and non-linear forces is not significant. The vertical force is almost constant over the entire frequency range for each amplitude, and judging by the distance between each curve, it appears that the increase in vertical force is approximately proportional to the increase in wave amplitude.

In terms of connecting the foil to a vessel, this scenario is of interest. The presence of a passive foil will apparently deliver approximately the same resultant force over a large frequency range.

Figure 12 shows how the thrust coefficient varies with amplitude and frequency. The thrust increase is not proportional to the amplitude increase. In fact, it is reasonable to estimate that the thrust is approximately proportional to the square of the wave amplitude: the thrust is proportional to the square of the angle of attack, and thus roughly proportional to the square of the vertical velocity over the foil.

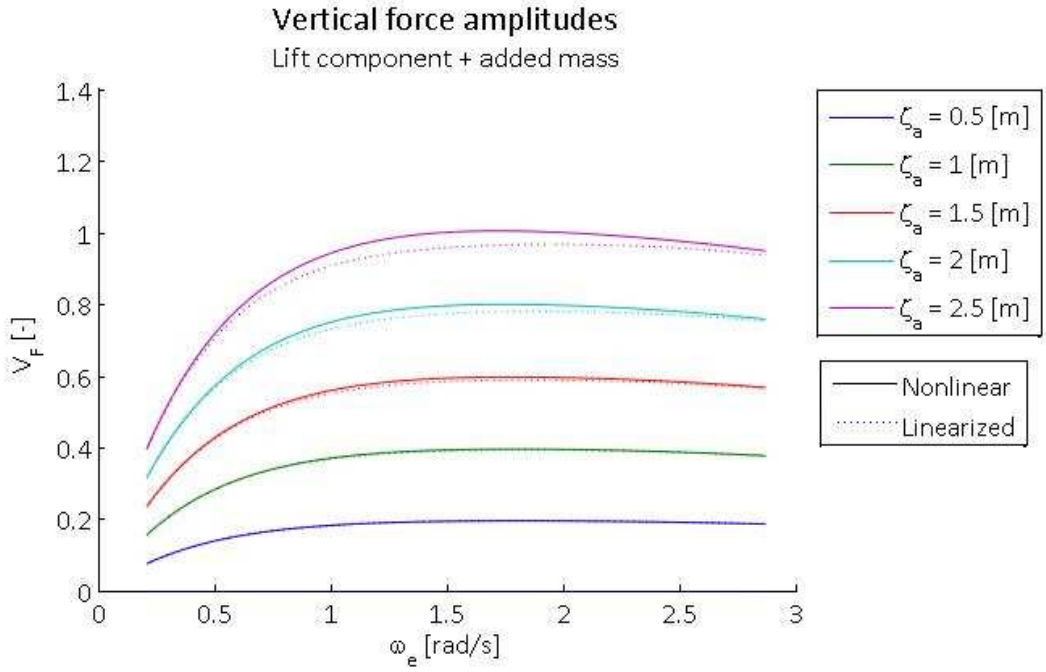

Figure 11: Case 1 - Vertical force coefficients on a passive foil in waves for wave amplitudes from 0.5 to 2.5 [m]. Nonlinear and linear.

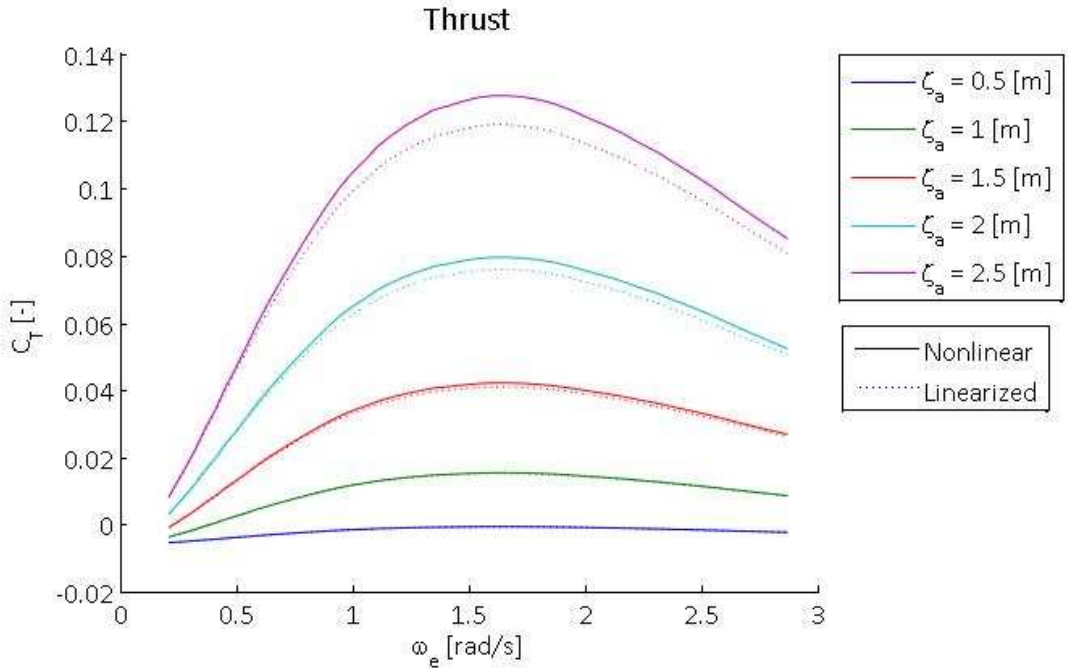

Figure 12: Case 1 - Thrust coefficients on a passive foil in waves for wave amplitudes from 0.5 to 2.5 [m]. Nonlinear and linear.

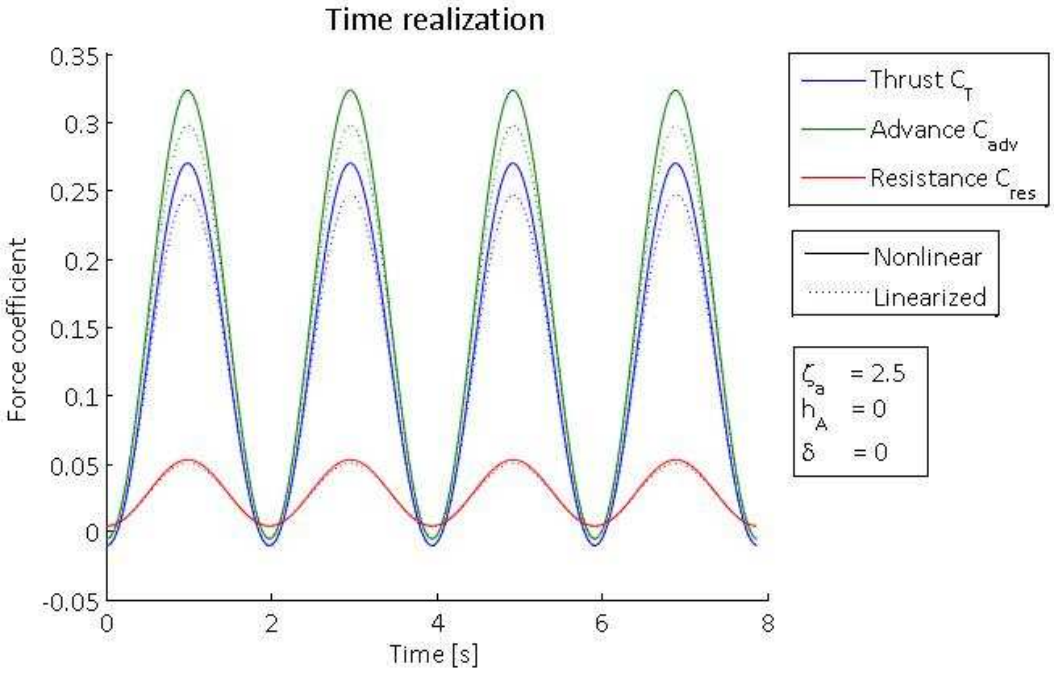

Figure 13: Case 1 - Example of time realization of horizontal force coefficients for a passive foil in waves of amplitude 2.5 [m].

Frequencies below $\omega_e = 0.9$ are of little interest, because they deliver little thrust. The most interesting frequency range for Case 1 is $0.9 < \omega_e < 2.5$, where the thrust coefficient is above 0.1.

Figure 13 exemplifies the realisation of thrust, advance and resistance in time. They are all in phase with each other, which they are for all frequencies.

Note that while the linear equations overpredict the angle of attack, they underpredict the thrust and vertical forces. This may have to do with that the resistance term in the thrust is proportional to the square of the angle of attack. Why linearization underpredicts the vertical force has not been studied.

Note that the minima of the time dependent advance in Figure 13 are less than zero. This is not possible according to the definition in equation (3.46). The reason for this error in the model has not been found.

Case 2: Foil with pitch oscillation in waves

In this scenario, the foil propagates with a constant velocity in an oscillating flow field. The pitch is adjusted so that the amplitude of the effective angle of attack is 15° for all frequencies. The effect of this can be seen in Figure 14, where the quasi-static lift coefficient remains constant for all frequencies. As for case 1, the unsteady lift reduces quickly with increasing frequency.

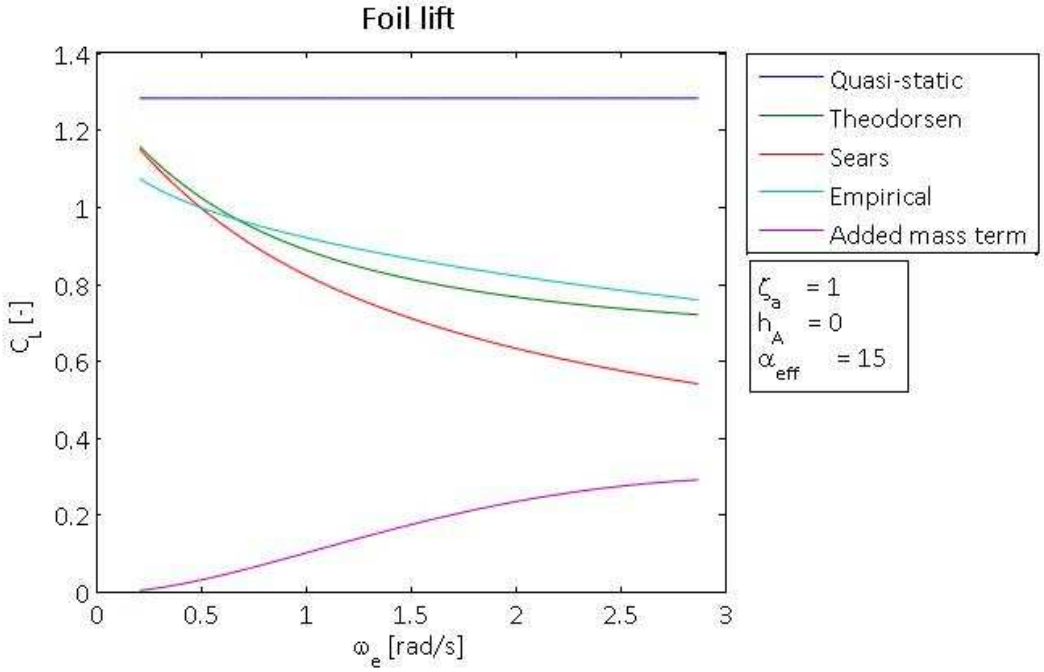

Figure 14: Case 2 - Steady and unsteady lift forces on foil oscillating in pitch in waves of height 1m. The added mass force has been included in magenta.

The difference in terms of increased lift compared to Case 1 is evident. This results in exactly the opposite phenomenon present in Case 1 for low frequencies: the vertical forces increase for low frequencies. The thrust has also increased somewhat for larger parts of the frequency range compared to Case 1.

Neither in this case is there a significant difference between linear and non-linear results. The largest difference for the thrust is 6.67%.

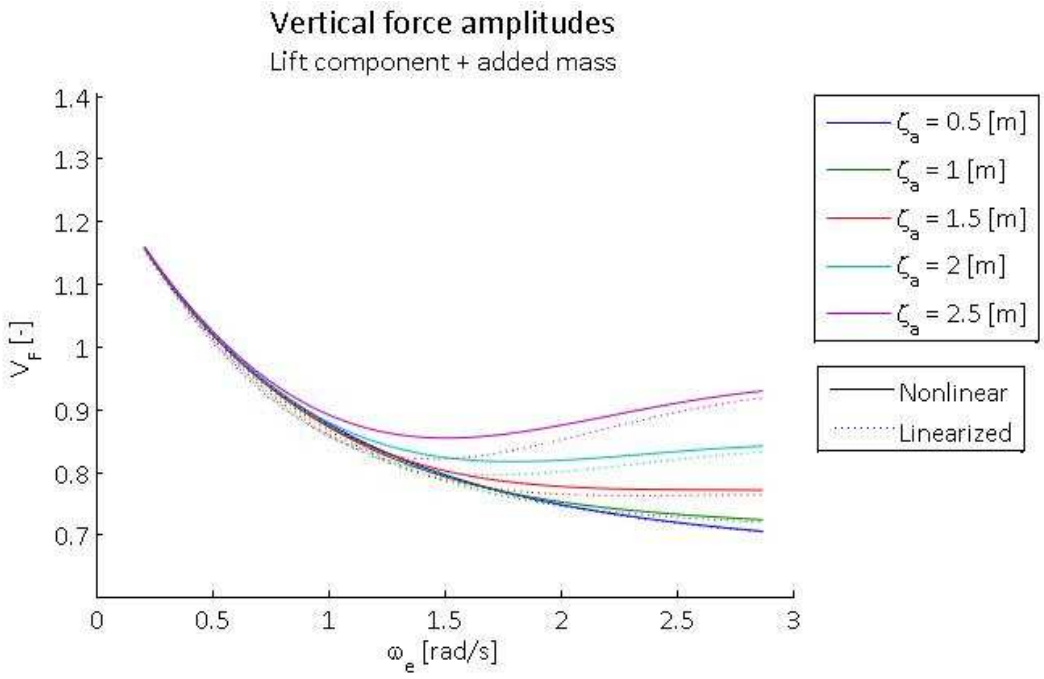

Figure 15: Case 2 - Vertical force coefficients on a foil oscillating in pitch in waves for wave amplitudes from 0.5 to 2.5 [m].

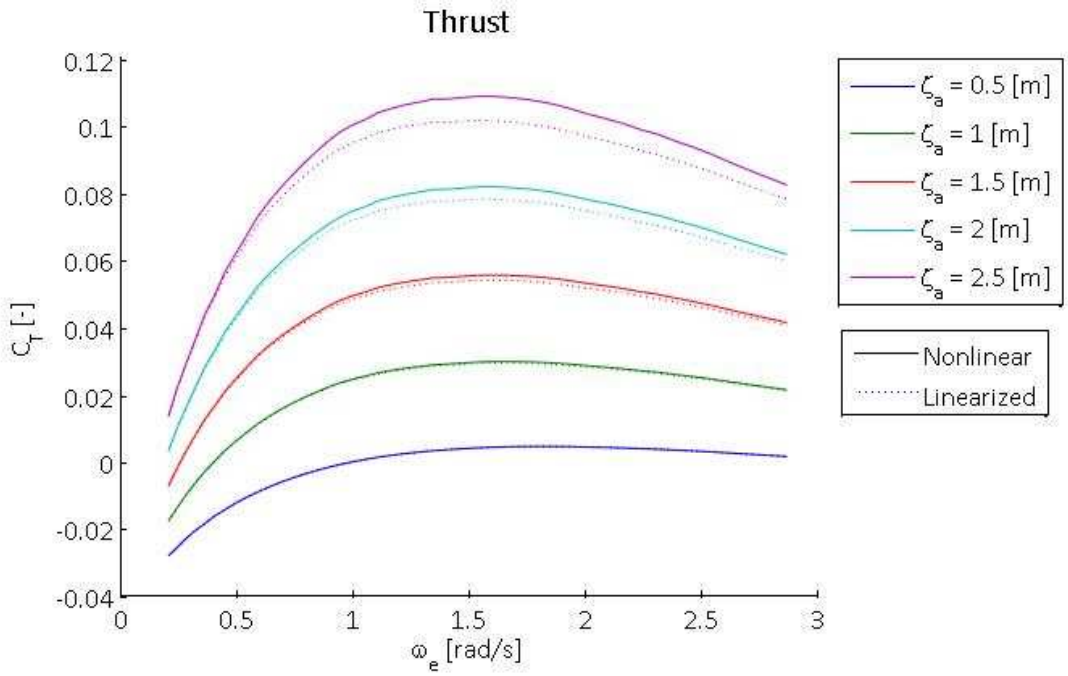

Figure 16: Case 2 - Thrust coefficients on a foil oscillating in pitch in waves for wave amplitudes from 0.5 to 2.5 [m]. Nonlinear and linear.

Case 3: Foil oscillating in heave only

In this case, the foil oscillates in heave and the pitch is zero. The heave amplitudes are identical to the wave amplitudes from cases 1 and 2. Thus, for increasing oscillation frequencies, the effective angle of attack will increase. For a given amplitude, when the frequency has increased until $\alpha = 15°$, the amplitude is reduced in order to avoid stall. As a consequence, all involved angles are small and the difference between linear and non-linear expressions are small: the largest difference between linearized and non-linear thrust is 4.8%, and for the vertical forces the difference is even less: 3.4%

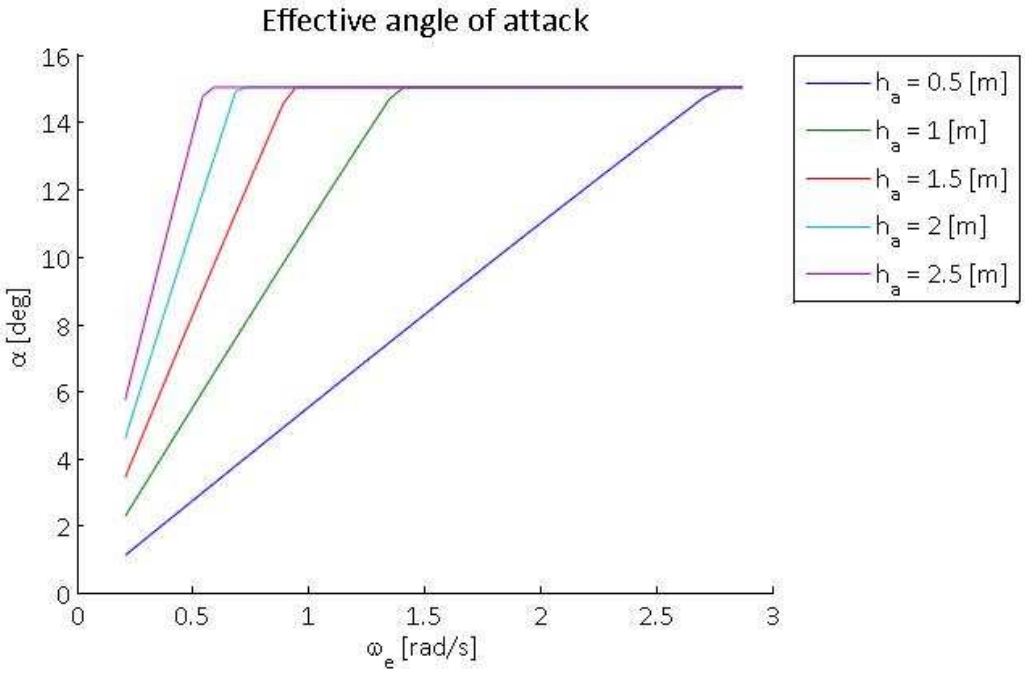

Figure 17: Case 3 - Angle of attack for a foil oscillating in heave for heave amplitudes spanning from 0.5 to 2.5 [m]. The amplitude is corrected for so that the angle does not exceed 15°. Therefore, the legend in the right part of the figure indicates the initial amplitude only.

Figure 18 shows how the heave amplitude varies in order to keep the angle of attack below stall angle. The different curves represent the different initial amplitudes.

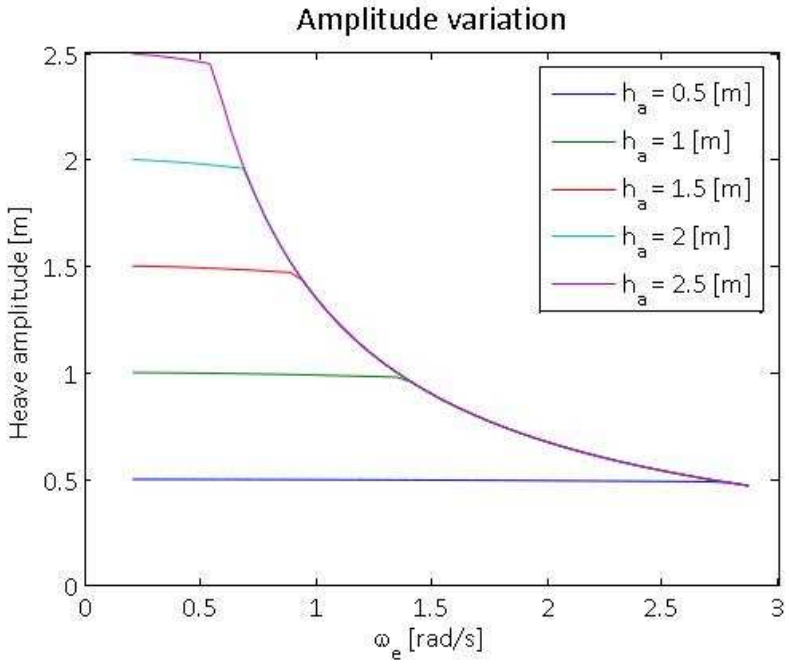

Figure 18:Case 3 - Heave amplitude variation of the oscillating foil described on page 39. The initial amplitudes are displayed in the color legend to the right.

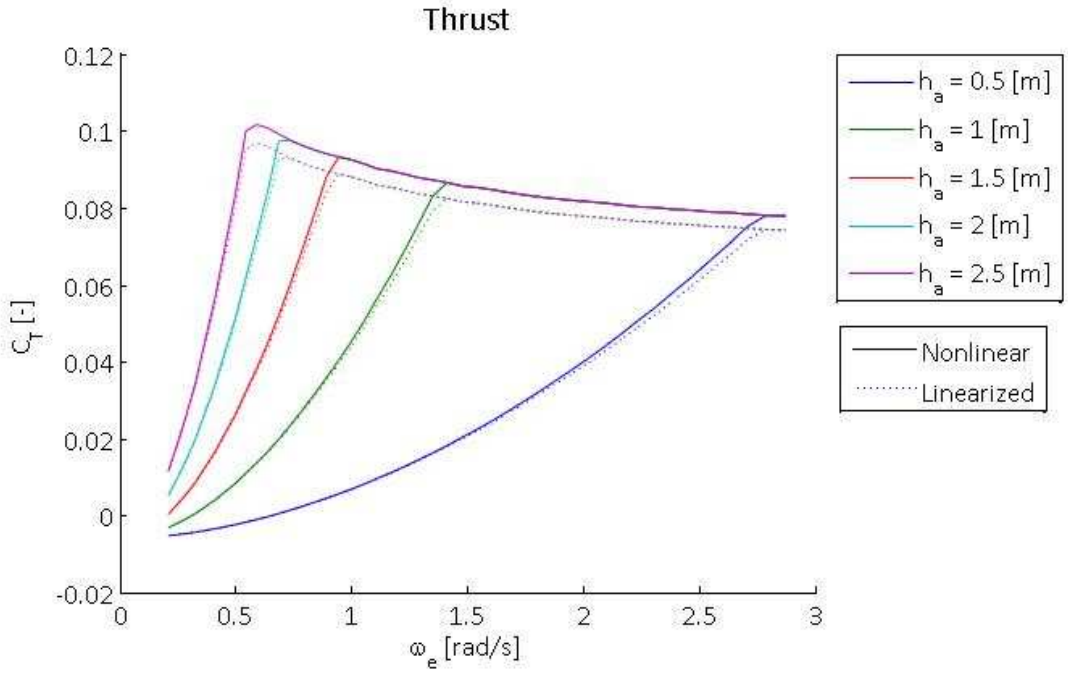

Figure 19: Case 3 - Thrust force of a foil oscillating in heave.

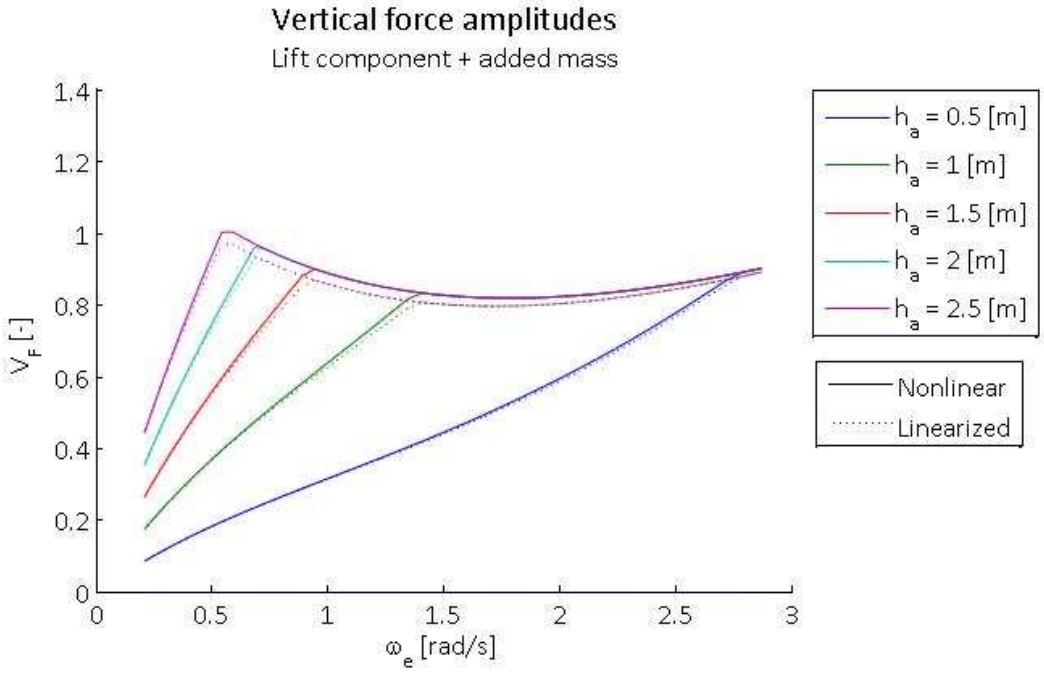

Figure 20: Case 3 –Vertical force amplitudes for a foil oscillating in heave for heave amplitudes spanning from 0.5 to 2.5 [m].

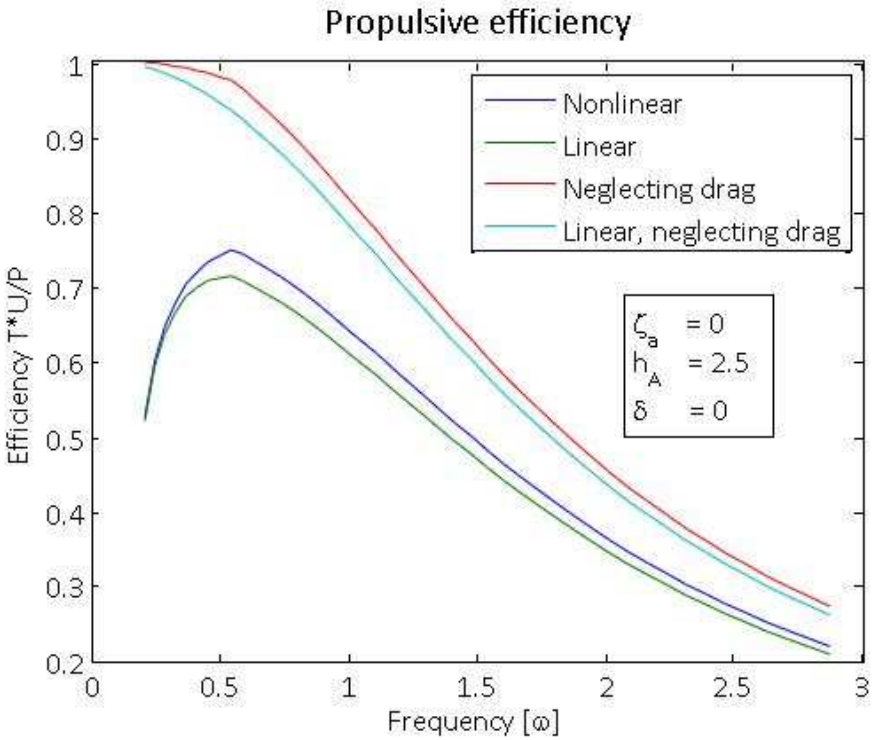

Figure 21: Case 3 –Propulsive efficiency, with and without drag, of foil oscillating in heave.

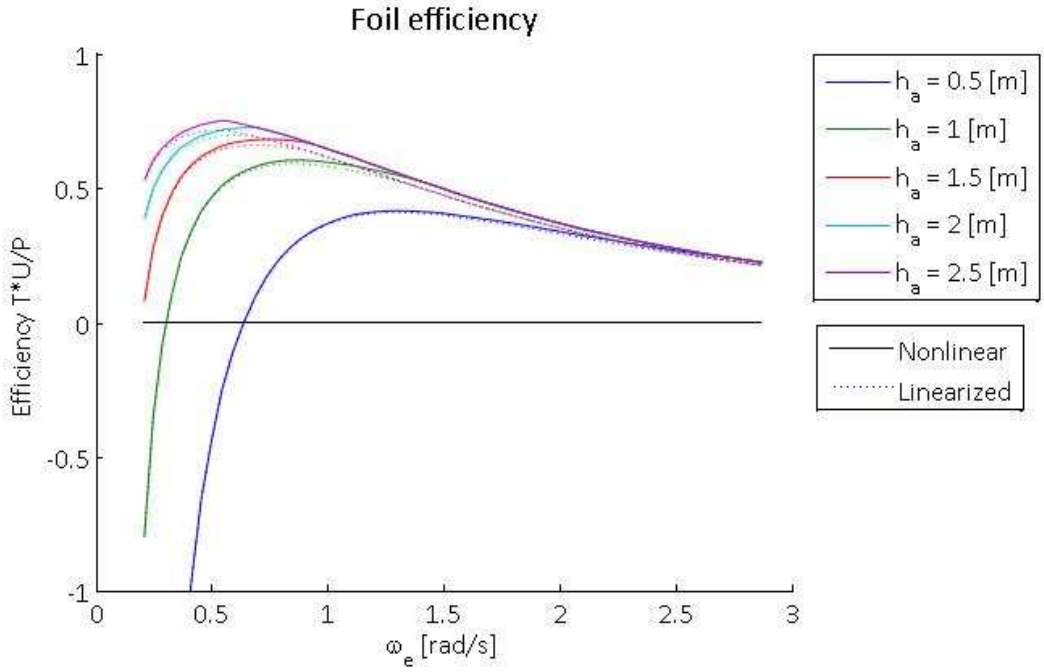

Figure 22: Case 3 – Propulsive efficiency foil oscillating in heave for heave amplitudes spanning from 0.5 to 2.5 [m]. The fact that the efficiency can be negative is due to that the resistance is larger than the advance for certain amplitudes and frequencies.

Figure 19 shows how the thrust varies with amplitude. It shows that for a foil employing an amplitude of 2.5 [m] will create significant thrust over much of the frequency range.

Since this case involves active heave motion of the foil, it is of interest to discuss the propulsive efficiency of this type of oscillation. Figure 21 shows that there is some deviance between the efficiency and the linearized efficiency, but the trends are evident. The advance efficiency terms where the drag contribution is neglected is included to verify that the 2D inviscid efficiency will approach unity for decreasing frequencies. Comparing Figure 21 with Figure 19 it becomes clear that this case has one major advantage: the largest thrust and the highest efficiency both occur within a very narrow frequency range.

Figure 22 shows that this case will produce thrust with efficiencies above 50% for frequencies up to $\omega_e = 1.5\left[rad/s\right]$

Case 4: Foil oscillating in heave and pitch

Experiments performed by Anderson et al. suggest that the optimal phase between heave and pitch is not 90 deg, but closer to 70 deg. Throughout this thesis, however, is assumed a 90 deg

phase for mathematical consistency in the simple models applied. As for case 3, the pitch angle is adjusted so that the effective angle of attack amplitude always will be $15°$.

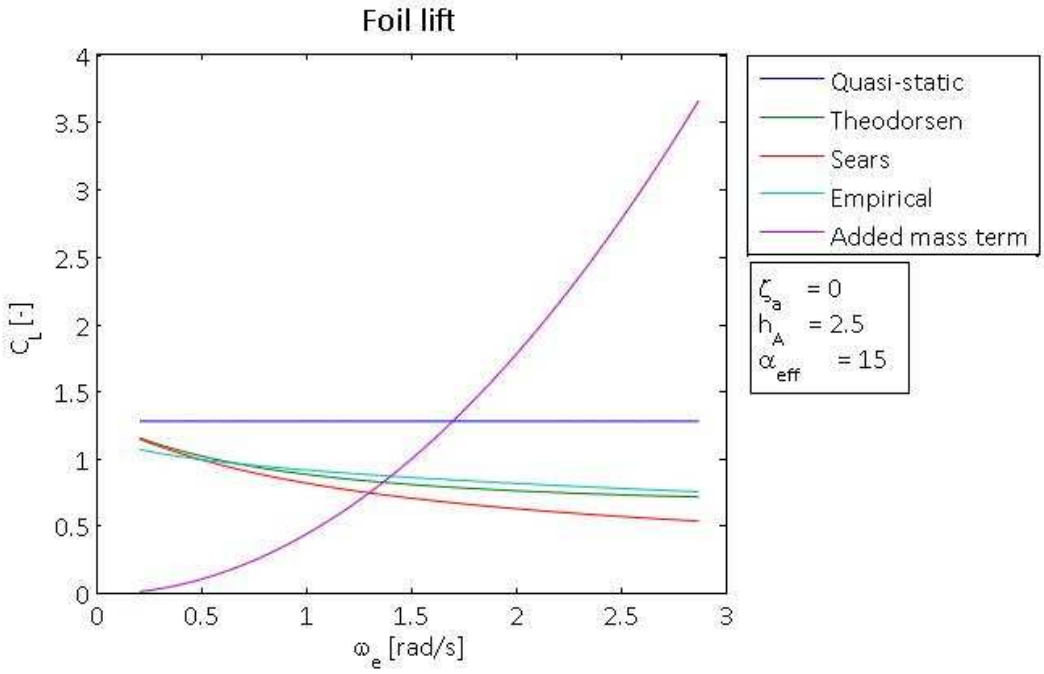

Figure 23: Case 4 – Lift force of a foil oscillating in heave and pitch. Added mass is included in magenta.

Figure 23 shows that the added mass equals the unsteady lift force in magnitude at $\omega_e \approx 1.4$. For smaller amplitudes, this crossing point is shifted to the right. However, as Figure 27 shows, the efficiency does not increase for smaller amplitudes even though the lift-to-added-mass ratio increases. The reason is that at lower amplitudes, the angle φ will be smaller and the advance term correspondingly smaller too, while the resistance term will be relatively larger. Advance and resistance curves can be found in Appendix 3.

Figure 24 shows that case 4 is the only case which displays significant resistance to linear methods. However, up to the point where linear and nonlinear theory differ significantly, this case provides high thrust for relatively high efficiency.

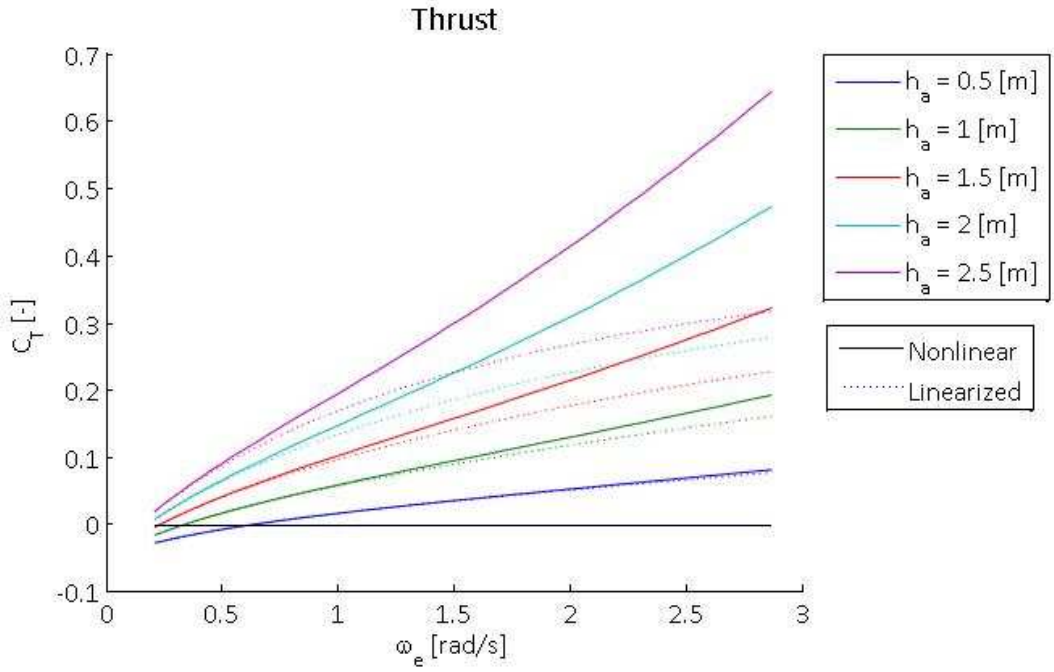

Figure 24: Case 4 - Thrust force of a foil oscillating in heave and pitch

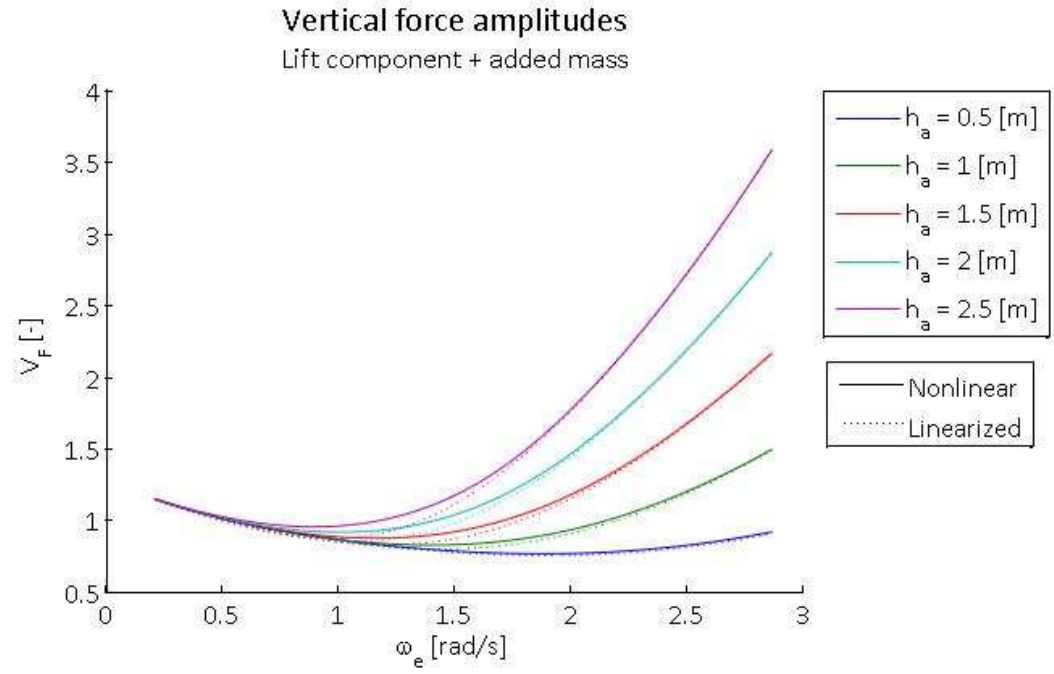

Figure 25: Case 4 –Vertical force amplitudes for a foil oscillating in heave and pitch for heave amplitudes spanning from 0.5 to 2.5 [m].

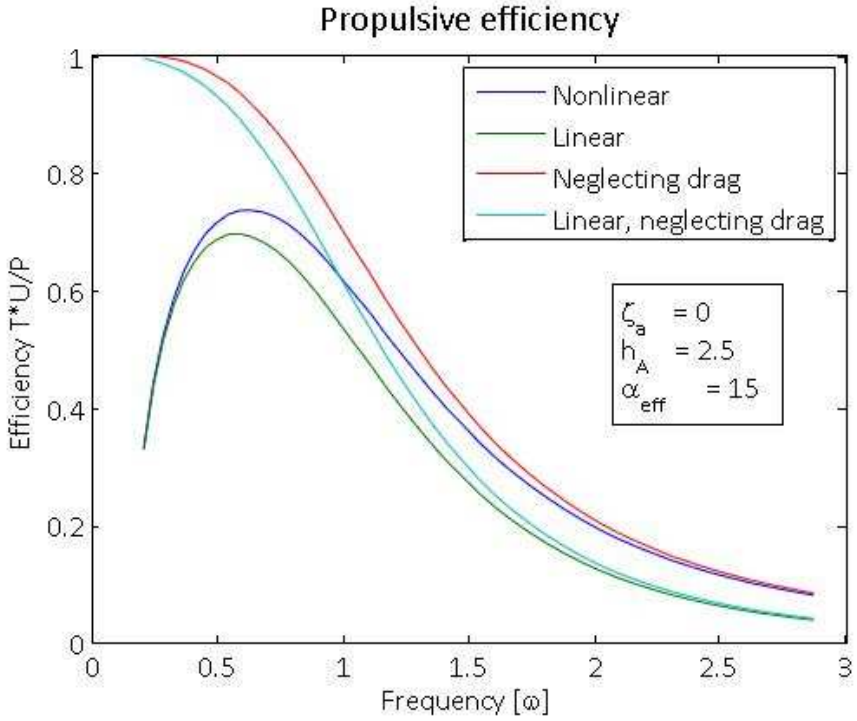

Figure 26: Case 3 –Propulsive efficiency, with and without drag, of foil oscillating in heave and pitch

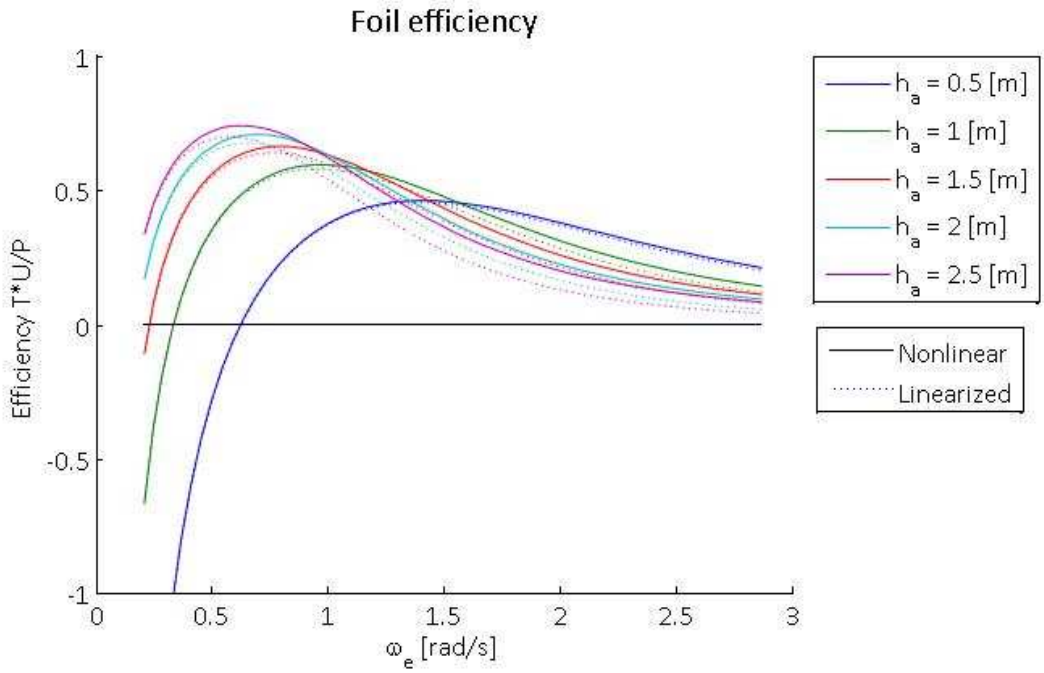

Figure 27: Case 4 – Propulsive efficiency foil oscillating in heave and pitch for heave amplitudes spanning from 0.5 to 2.5 [m].

Preliminary conclusions

The difference between the quasi-steady and unsteady lift forces are aparent already for quite low frequencies. However, the for most cases the differences were not too significant to see evident trends compared to the original equations.

One interesting observation is that the active oscillating foils produce best results in terms of efficiency with high thrust coefficients for frequencies between 0.5 and 1 [rad/s] approximately, while the foil in waves produce highest thrust for frequencies between 1 and 2.5 [rad/s].

For all cases, the vertical forces were approximately an order of magnitude larger than the thrust force. Whether large vertical forces is a problem or not depends on how the foil is intended to be used. When the foil is connected to a vessel, large vertical forces may be beneficial in terms of pitch reduction. This has been discussed by both Borgen (2010) and Eitzen (2012). However, when applying vertical forces to the foil in order to generate forward thrust, large vertical forces are not beneficial.

Note that the efficiency can be negative for low frequencies, where the resistance is larger than the advance.

The calm water resistance of the vessel considered in chapter 4.2 is $R_{TS} = 157.09e^3\ [kN]$. Non-dimensionalized by the same factor as the foil forces studied in this thesis, the vessel resistance coefficient becomes:

$$C_{RTS} = \frac{157.09e^3}{\frac{1}{2}\rho c s U^2} = 0.184$$

In case 3, a thrust coefficient of $C_T = 0.1$ is achieved at an efficiency of $\sigma = 0.75$. In case 4, a thrust coefficient of $C_T = 0.2$ is achieved in the region where the difference between linear and nonlinear theory starts to be significant. The efficiency is $\sigma = 0.57$.

This indicates that two or more foils are necessary in order to achieve enough thrust to propell the vessel.

Advance and resistance coefficients for each case study can be found in Appendix 2.

4.2 Ship model

The vessel applied in this study is a Rolls-Royce UT751E design platform supply vessel. The main dimensions, and loading and environment conditions are given in Table 4.

L_{PP}	80.8	$[m]$
B	21	$[m]$
T	6.8	$[m]$
COG	36.47	$[m]$ rel.AP
Δ	8985.2	$[mton]$
U	10	$[kn]$
R_{TS}	157.09	$[kN]$
Wave heading	*Head sea*	

Table 4: Vessel and environment data

Complete data regarding vessel characteristics, loading condition and environment can be found in the VERES files attached to this thesis.

4.2.1 Time domain

(Eitzen 2012) created time domain models of the coupled vessel-foil system. The results were apparently accurate, but attempts to apply Eitzen's models to the same case vessel with a passive foil loaded at another draught gave large discrepancies between time- and frequency domain results. The models were complicated and not well documented.

Inspired by this, attempts were made to create simple time domain models that applied Cummins equation and a state space approximation for the fluid memory term. Two models were created: one applying pure frequency domain coefficients in a time domain solution, and the other applying Cummins equation. The first became unstable for frequencies lower than 0.4 [rad/s], and the second was apparently too simple: low frequency results were relatively good, but large differences appeared for frequencies higher than approximately 0.4 [rad/s].

Thus, combining the two models, the frequency responses in heave and pitch were estimated in the time domain. This can be seen in Figure 28 and Figure 29. The transition from the Cummins

model to the frequency domain model can be seen in Figure 29 for $\omega = 0.4$. The Cummins model gave good results for pitch, but for heave there can be seen a deviation from the frequency domain results for low frequencies.

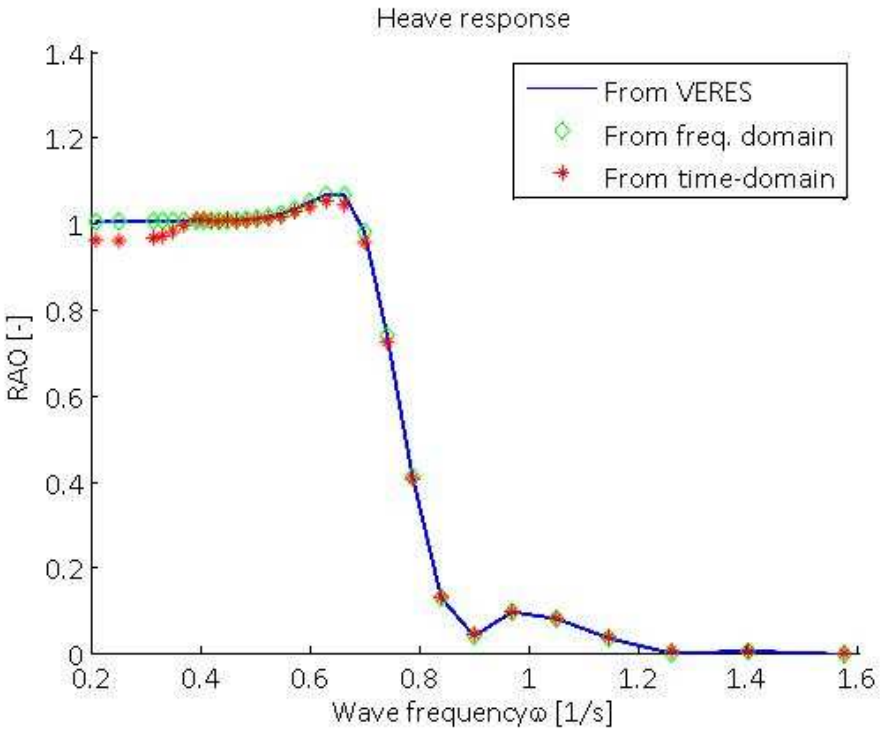

Figure 28: Heave response from Veres, own frequency domain calculations and time domain models

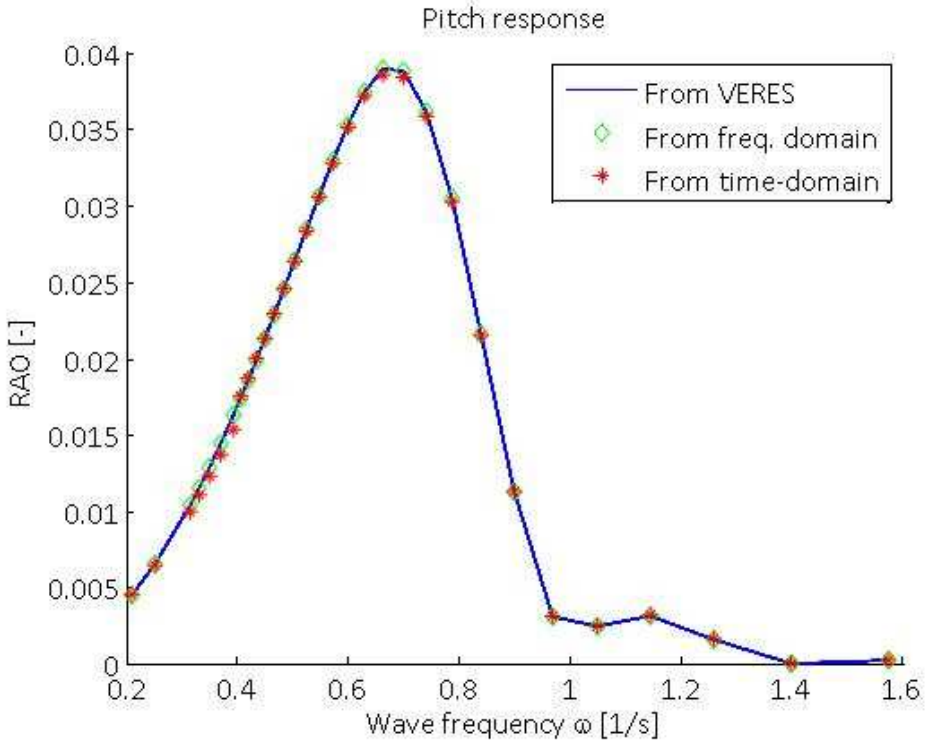

Figure 29: Pitch response from Veres, own frequency domain calculations and time domain models

4.3 Ship with foil

4.3.1 Preliminary thought

For the theory describing vessel response in the frequency domain when the vessel is connected to a passive foil, please refer to (Fathi) and (Eitzen 2012). Some related concepts will be elaborated on in the following.

The linearized angle of attack for a foil connected to a vessel is defined as

$$\begin{aligned}\alpha_e &= \frac{-\dot{z}}{U} - \delta \\ &= \frac{1}{U}\left(w - \dot{h} - \dot{\eta}_3 + x_f\dot{\eta}_5 + U\eta_5\right) - \delta\end{aligned}$$

This can only be incorporated in a frequency domain approach when all terms are linear. For a passive foil in waves, this is not a bad assumption, as described in the case studies above. For an active foil, however, large angles may arise, rendering linearization impossible. The coupled vessel-foil study performed here may therefore be superficial.

4.3.2 Verification against VERES

Hydrodynamic coefficients for the case vessel described above were found in ShipX. These were applied in frequency domain heave and pitch response calculations using MATLAB as a basis for developing a combined vessel-foil model. The theory applied in the calculations is the same thas is supplied in the software documentation (Fathi 2010). However, the calculated responses were not identical to the response output from ShipX. The results can be seen in

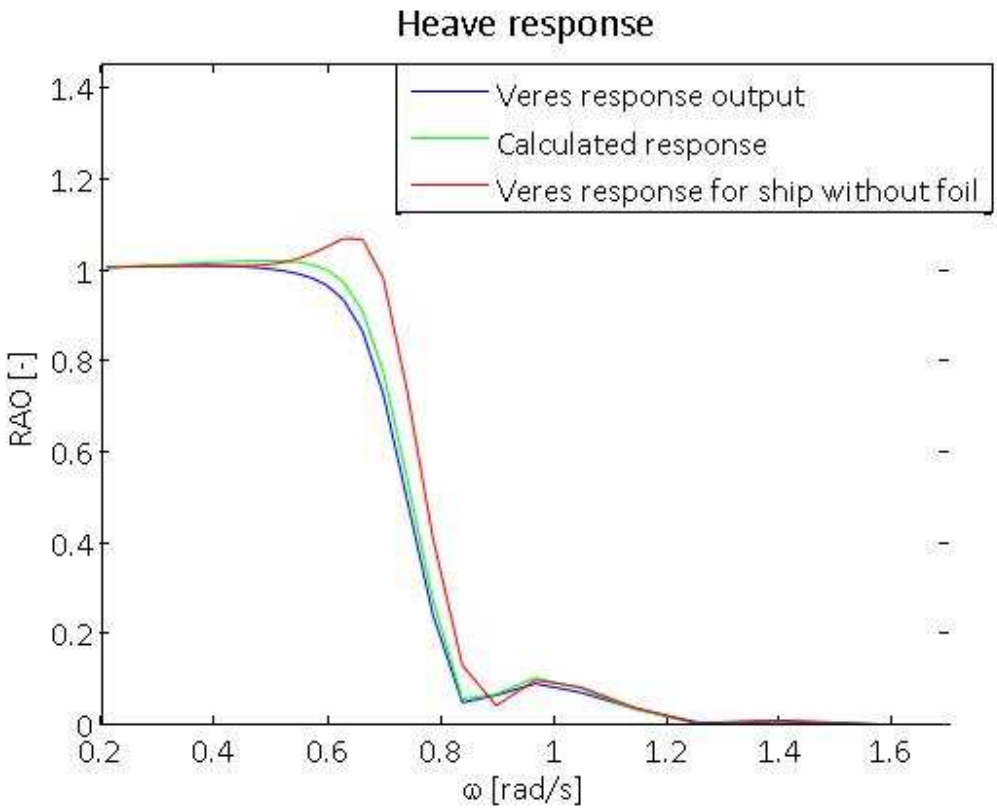

Figure 30: Heave response of the case vessel with a passive foil. Considereing that the theory behind the two calculations should be identical, the discrepancies are large. Also included is the response for a vessel withouth foil.

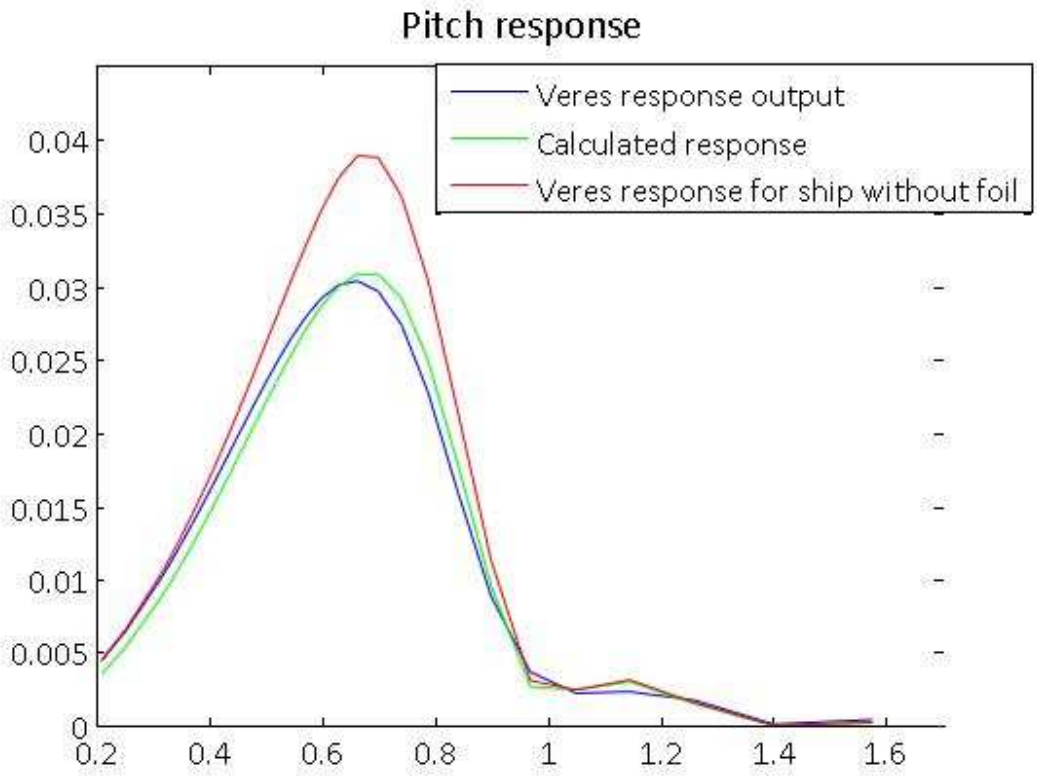

Figure 31: Pitch response of the case vessel with a passive foil. Considering that the theory behind the two calculations should be identical, the discrepancies are large. Also included is the response of the case vessel without a foil.

4.3.3 A comment on foil location

Assume vessel pitches about COG.

Intuitively, to capture the vessel pitch motion in the angle of attack, it will be appropriate to place the foil either in the bow or in the aft region of the vessel. Close to the center of rotation, the local vertical velocities of the ship are small, and placing the foil here will not be likely to extract as much wave energy as when the foil is located where the vertical velocites are larger.

Only the magnitude and not the phase angle of the vertical water velocity will vary with depth. Under the superficial simplification that larger velocities create larger angles of attack, the foil is placed as close to the surface as deemed suitable, and the effect of depth variation is not studied

in this report. Nonetheless, some possible advantages of placing the foil at a greater depth are mentioned:

- At greater depths, the wave components with higher frequencies will not affect the angle of attack. Therefore, in an irregular sea state, the high frequencies do not need to be filtered out in a real-time control system.
- In an irregular sea state, the incoming waves are of a random nature, and the depth variation of the foil will thus be unknown a priori. Thus, by placing the foil at a greater depth, the risk of slamming may be reduced.

Advantages of placing the foil aft:

- The resulting jet is not sent directly into the bow but behind the vessel
- Probes or sensors can be placed along the vessel sides and in the bow to estimate the sea state. Together with a model of the flow field set up by the ship, the angle of attack of the foil can be estimated or optimised.

5 Conclusions and discussion

The advantages of oscillating the foil at low frequencies are several, both in terms of physical benefits and modeling benefits:

- The efficieny is higher due to small losses in added mass
- The pitch oscillation angles of the foil are limited to smaller angles. With regard to the large forces involved, this requires a robust system. This may be simpler to construct when the angles are limited to small amplitudes than a foil which has to be controlled over a large angular range.
- Lower frequencies will result in lower fatigue due to reduced number of cycles. Higher order resonant frequencies that will appear must be studied in this perspective.
- The equations may be linearized
- Uncertainties regarding use of linear theory is reduced

It will likely be necessary to construct a system consisting of two or more foils. Including a passive foil above or behind the active foil may increase efficiency even more due to wing-on-ground effects and capture of wake vortices, respectively. In terms of construction and costs, this should not represent a big issue: once an active foil system is designed and paid for, contructing a system including an active and passive foil should be both mechanically and economically feasible. Also, with two foils, one has more options regarding pitch damping than with one foil alone, because the second foil may be adjusted so that vertical forces cancel each other.

Introducing a second foil will, however, also introduce very complicated flow physics: the troubles that arise when combining 3D steady theory with 2D unsteady theory will now be accompanied by interaction effects between the foils. And even then one has not considered the effect of the hull proximity.

Linear theory and rules of thumb are necessary to understand the basic dynamics of foil theory, and may be applied to perform simple calculations and estimate trends. But if the dynamics of a two-foil propulsor is to be studied with the aim that it is to be constructed at some point, computer simulations must resort to panel codes or other numerical solvers. Even with the use of more advanced numerical solvers, it may however still turn out that viscous and pressure forces can be studied separately, and this will probably be advantageous. The best results, however,

would be achieved by gathering 50 or so master and bachelor students, buying an old fishing or offshore vessel, and perform model tests when the seas are calm or long-crested.

Regarding combined heave and pitch oscillation:

- Due to the time varying forces on the foil, a time-varying moment will be set up about the connection point, also for the case where the foil does not oscillate in pitch. In order to control the angle of attack, an active pitch angle control mechanism must therefore be implemented. Thus, studying a configuration where the foil only oscillates in heave will simplify the modeling, but does not provide any simplification to the actual system that is to be built.

A properly working time domain model will be much better suited for studies of a combined foil-vessel system. This is also a conclusion advocated by Eitzen (Eitzen 2012), who studied active pitch control. A time domain model will allow for non-linearities and feedback. Also, when studying the system in irregular seas, accurat control of the angle of attack is necessary. Due to the randomness in time regarding the phase angle between the wave components, this is not possible in the frequency domain.

6 Recommendations for further work

Even though the author advocates working in the time domain, some features may still be interesting to study in the frequency domain: Refine foil motion to square wave:

- Keep heave velocity and pitch angle constant for say 80% of the double heave amplitude. This way the angle of attack remains at max for much longer stretches of time. Also, the foil accelerations occur only at the top and bottom of the trajectory, condensing them in time and thus increasing in magnitude. The effect of this on the added mass must be studied, but perhaps the reduction in acceleration time and the shape of the wave function describing the acceleration can reduce the added mass for the foil for high frequencies. Note that this will influence the Theodorsen function, and one must consider if a modified version of the Theodorsen term is necessary.
- Introductory square wave tests can be performed in the frequency domain by expressing the motions as a Taylor series. For each frequency in the series, the Theodorsen function can be found and approximated with a state space model using the matrix fitting toolbox. The results can be superimposed and used in a time domain model.

In experimental studies of unsteady foils, the magnutide of the thrust produced is closely linked to the formation of a reverse Karman vortex street, where a jet flow occurs behind the foil. Experimental thrust optimization is therefore related to optimizing the wake pattern.

In theoretical studies, the vortices are aligned along the same horizontal line, and there is no jet creating a net thrust force. The thrust force is linked to the lift, which depends on the amplitude of heave and pitch, the phase between the two, the center of rotation on the foil, and frequency. Due to the imaginary term of the Theodorsen function, the phase of the unsteady part of the lift will vary with frequency, and this will cause a frequency dependent time lag between the angle of attack and the resulting force.

A comparison of the theoretical and experimental approaches, and how the thrust is optimized in each of them, may provide insight into the dynamics governing the system.

Garrick: the center of rotation influences the efficiency. How will this be affected when both the foil and the vessel rotates? When implemented in the time domain, Garrick's propulsion formula must probably be approximated using a curve-fitting tool.

Create or obtain simple panel codes for an oscillating foil. Envision a panel code where the input is a numeric array defining the foil motion in time and the output is an array describing the resultant forces and moments in time. If the inputs are given in real time and not as a predefined motion, this can be implemented in a time domain model of a coupled vessel-foil system. The output from the panel code can be fed back to the exciting forces in the linear vessel response equations.

7 Summary of assumptions and simplifications

In addition to the common assumptions regarding inviscid, irrotational and incompressible flow, linearity and superposition of contributions from pressure and viscous effects, the following have been assumed in these models.

- The foil has an elliptical planform area, and the mean chord length is used in the calculations.
- The NACA 0012 empirical viscous lift-drag curve is assumed applicable for unsteady theory.
- The assumptions that the potential and viscous drag are in phase with the lift have not been verified.
- The 3D lift coefficient given in equation (3.15) is assumed valid for this foil. The foil studied in this project has an aspect ratio of 7. (Faltinsen 2005) notes that the error for a foil with $\Lambda = 8$ is 5% for steady flow. How the unsteady flow will affect the goodness of the definition is unknown.
- The effect of rotational velocity in equation (4.1) has been neglected.
- Damping forces have been neglected.
- The Theodorsen function is applied to both the oscillating foil problem and the sinussoidal gust problem. In a strict sense, the Sears function should be applied to the latter.
- The time-dependency of the foil added mass for large equations is neglected.
- The foil added moment (rotational added mass) is neglected.
- It is assumed that the Theodorsen function is valid for large angles as long as the effective angle of attack is small.
- The drag contribution to the vertical force is neglected.
- The definition of propulsive efficiency includes only the vertical input force and not the input moments and other effects that will have an effect on the value.

8 Recommendations for students approaching this topic

Study Fridtjof Eitzen's master thesis (Eitzen 2012). He provides a solid theoretical foundation for tools that may be of assistance in approaching this topic. Keep in mind that both his argumentation and his MATLAB code can be quite inaccessible at times, especially for one not familiar with the theory and notation applied in control engineering. However, his sources are readily available, as is the academic environment at the Marine Technology Cente.

The assumptions, results and discussions in this thesis may be of interest. If that is the case, Appendix 2 may be of value for understanding or reproducing simulation results.

It is, however, the author's opinion that one can delve deep into the details of the frequency domain approach without gaining any significant knowledge compared to what can be achieved by studying and applying the time domain approach. Frequency domain solutions can be used for verification, but keep in mind that the more involved the time domain model becomes, the less relevant the frequency domain models becomes.

Also, it may be an advantage to become familiar with SIMULINK, state space modeling, and Cummins equation and how to model this in time.

Should a reader have questions regarding material presented in this report, feel freet to contact the author at jacob.hauge@outlook.com.

References

Abbott, I. H. and A. E. v. Doenhoff (1959). Theory of wing sections: including a summary of airfoil data, DoverPublications. com.

Anderson, J. M., K. Streitlien, D. S. Barrett and M. S. Triantafyllou (1998). "Oscillating foils of high propulsive efficiency." Journal of Fluid Mechanics **360**(1): 41-72.

Borgen, C. T. (2010). Application of an active foil propeller. Master, Norwegian University of Science and Technology.

Breslin, J. P. and P. Andersen (1996). Hydrodynamics of ship propellers, Cambridge University Press.

Chopra, M. (1976). "Large amplitude lunate-tail theory of fish locomotion." J. Fluid Mech **74**(part I): 161-182.

De Silva, L. W. A. and H. Yamaguchi (2012). "Numerical study on active wave devouring propulsion." Journal of marine science and technology **17**(3): 261-275.

DeLaurier, J. D. (1993). "An aerodynamic model for flapping-wing flight." Aeronautical Journal **97**(964): 125-130.

Dimitriadis, G. "Lecture notes in Introduction to Aeroelasticity." from www.ltas-aea.ulg.ac.be/cms/uploads/Aeroelasticity01.pdf.

Eitzen, F. C. (2012). Mathematical Modelling of a Foil Propulsion System. Master, Norwegian University of Science and Technology.

Faltinsen, O. (1993). Sea loads on ships and offshore structures, Cambridge university press.

Faltinsen, O. M. (2005). Hydrodynamics of high-speed marine vehicles, Cambridge University Press.

Fathi, D. VERES Motion Control Theory Manual, MARINTEK.

Fathi, D. (2010). User manual - ShipX Vessel Responses. .

Fossen, T. I. (2011). Handbook of marine craft hydrodynamics and motion control, John Wiley & Sons.

Garrick, I. E. (1936). Propulsion of a flapping and oscillating airfoil, National Advisory Committee for Aeronautics.

Guglielmini, L. and P. Blondeaux (2004). "Propulsive efficiency of oscillating foils." European Journal of Mechanics-B/Fluids **23**(2): 255-278.

Gustavsen, B. (2009). Matrix Fitting Toolbox for rational modeling from Y-parameter and S-parameter data, Sintef Energy Research.

Jones, K. D. and M. F. Platzer (1999). An experimental and numerical investigation of flapping-wing propulsion. AIAA paper 99-0995.

Kármán, T. v. and J. M. Burgers (1935). Div. E. General Aerodynamic Theory - Perfect Fluids.

Kroo, I. (2007). "Lecture notes in AA200B Applied Aerodynamics II." from http://adg.stanford.edu/aa200b/lecturenotes/index.html.

Leishman, J. G. (2006). Principles of helicopter aerodynamics, Cambridge University Press.

Minsaas, K. and S. Steen (2008). Kompendium - Foil theory, Department of Marine Technology.

Naito, S. and H. Isshiki (2005). "Effect of bow wings on ship propulsion and motions." Applied Mechanics Reviews **58**: 253-268.

Newman, J. N. (1978). Marine Hydrodynamics. Cambridge, MIT Press.

Perez, T. and T. I. Fossen (2008). "Joint identification of infinite-frequency added mass and fluid-memory models of marine structures." Modeling, Identification and Control **29**(3): 93-102.

Perez, T. and T. I. Fossen (2009). "A matlab toolbox for parametric identification of radiation-force models of ships and offshore structures." Modeling, Identification and Control **30**(1): 1-15.
Rottmann, K. (2003). "Matematisk formelsamling." Bracan Forlag **2**.
Scherer, J. O. (1968). Experimental and Theoretical Investigation of Large Amplitude Oscillation Foil Propulsion Systems, US Army Engineering Research and Development Laboratories.
Sears, W. R. (1941). "Some aspects of non-stationary airfoil theory and its practical application." Journal of the Aeronautical Sciences (Institute of the Aeronautical Sciences) **8**(3): 104-108.
Steen, S. (2010). Foil theory 1: Circulation and lift. Lecture notes in TMR4220 Naval Hydrodynamics.
Theodorsen, T. (1934). General Theory of Aerodynamic Instability and the Mechanism of Flutter, NACA Report 496**:** 291-311.
Wolfram|Alpha. (2013). from www.wolframalpha.com/.

Appendix 1: NACA 0012

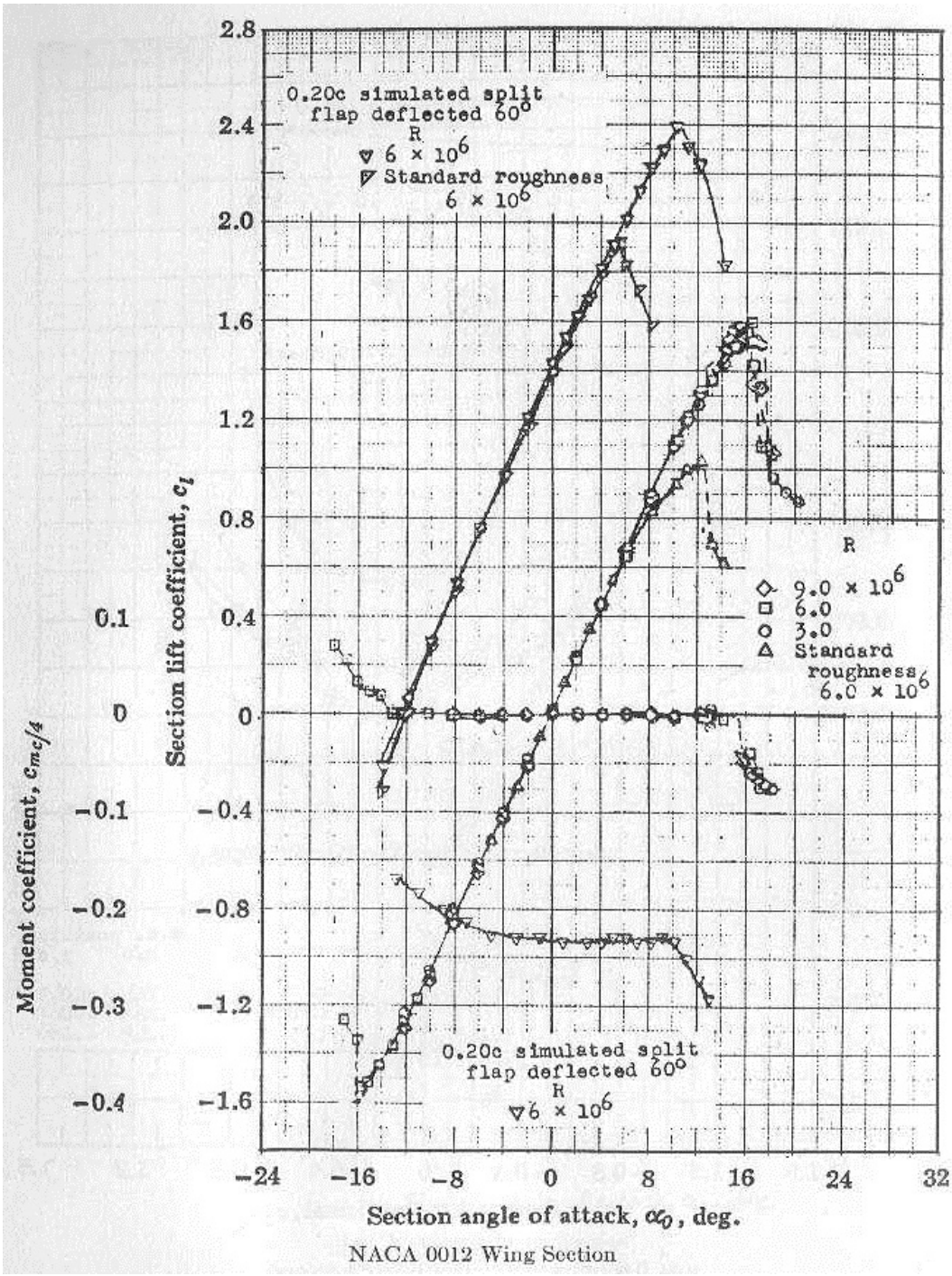

Figure 32: Relation between angle of attack and 2D lift for the NACA 0012 foil (Abbott and Doenhoff 1959)

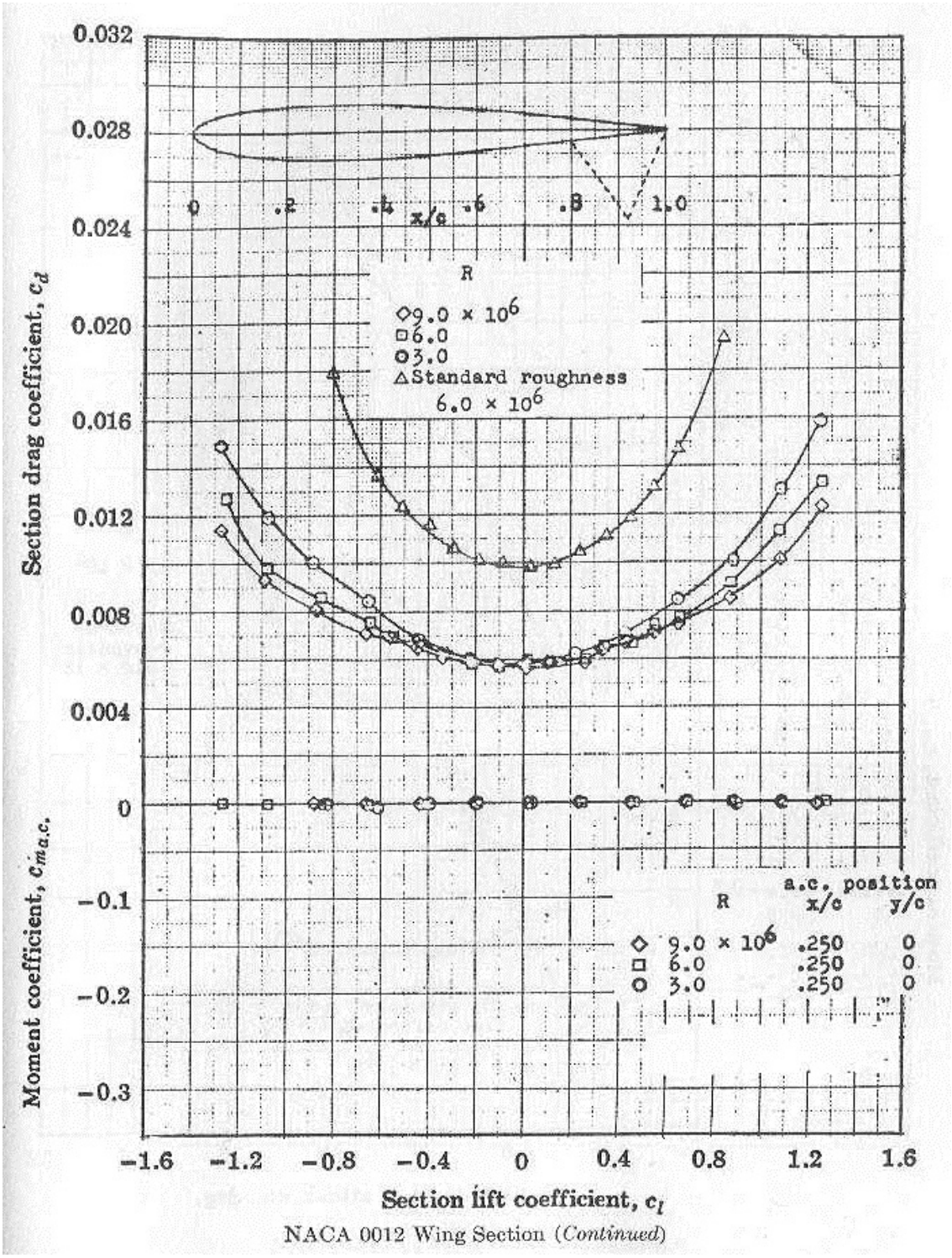

Figure 33: Relation between 2D lift and viscous drag for the NACA 0012 foil (Abbott and Doenhoff 1959)

Appendix 2: Advance and resistance coefficients from the foil model

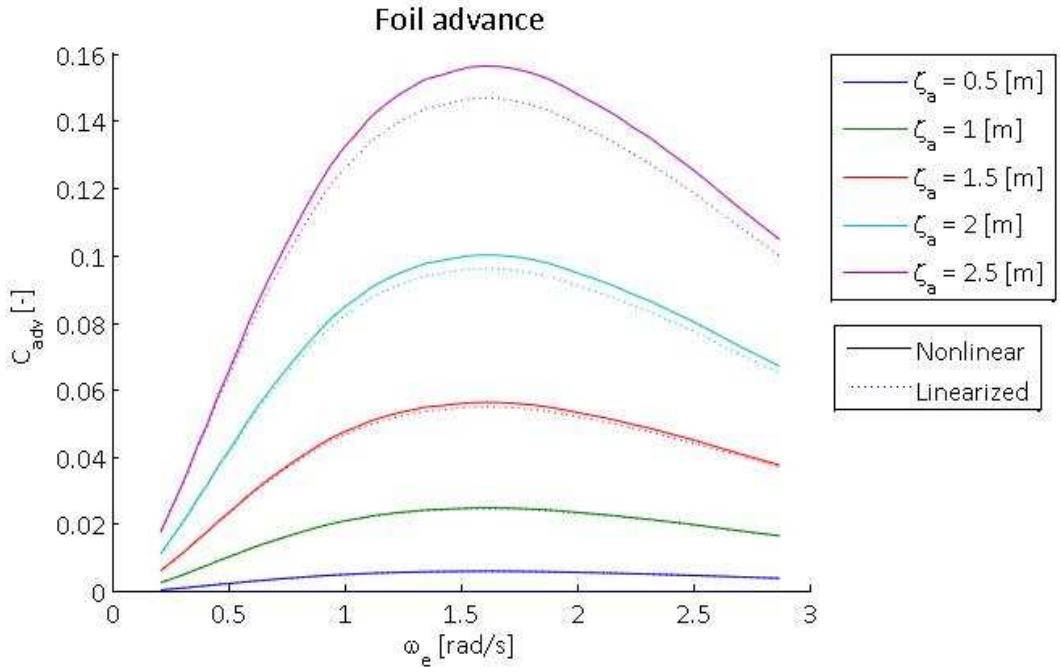

Figure 34:Case 1 advance coefficients for wave amplitudes from 0.5 to 2.5 [m]. Nonlinear and linear.

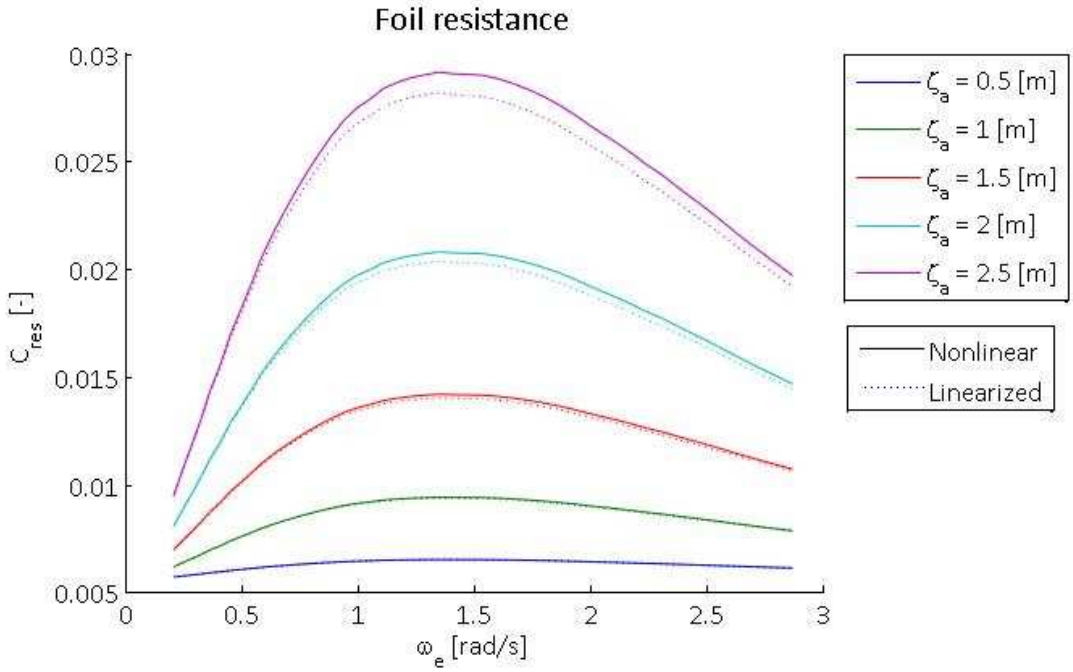

Figure 35: Case 1 resistance coefficients for wave amplitudes from 0.5 to 2.5 [m]. Nonlinear and linear.

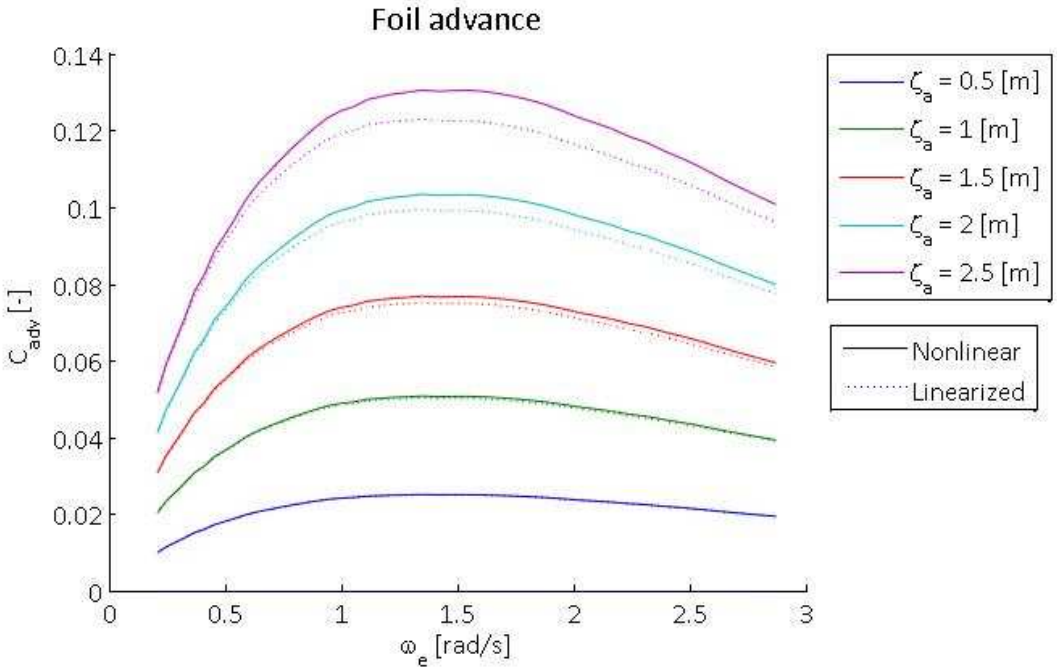

Figure 36: Case 2 advance coefficients for wave amplitudes from 0.5 to 2.5 [m]. Nonlinear and linear.

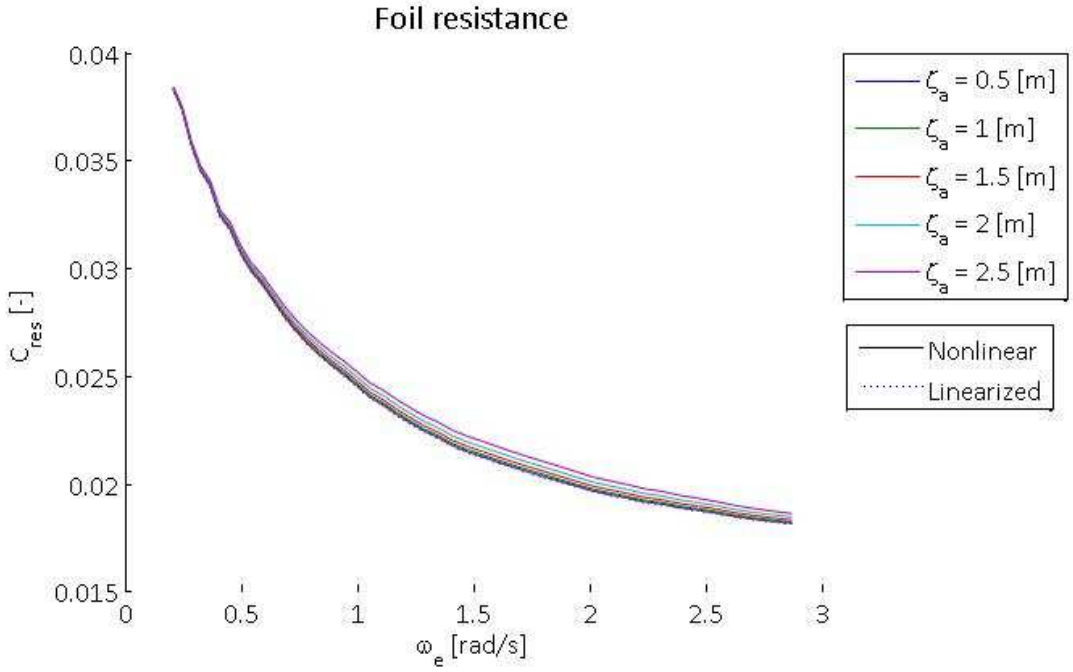

Figure 37: Case 2 resistance coefficients for wave amplitudes from 0.5 to 2.5 [m]. Nonlinear and linear.

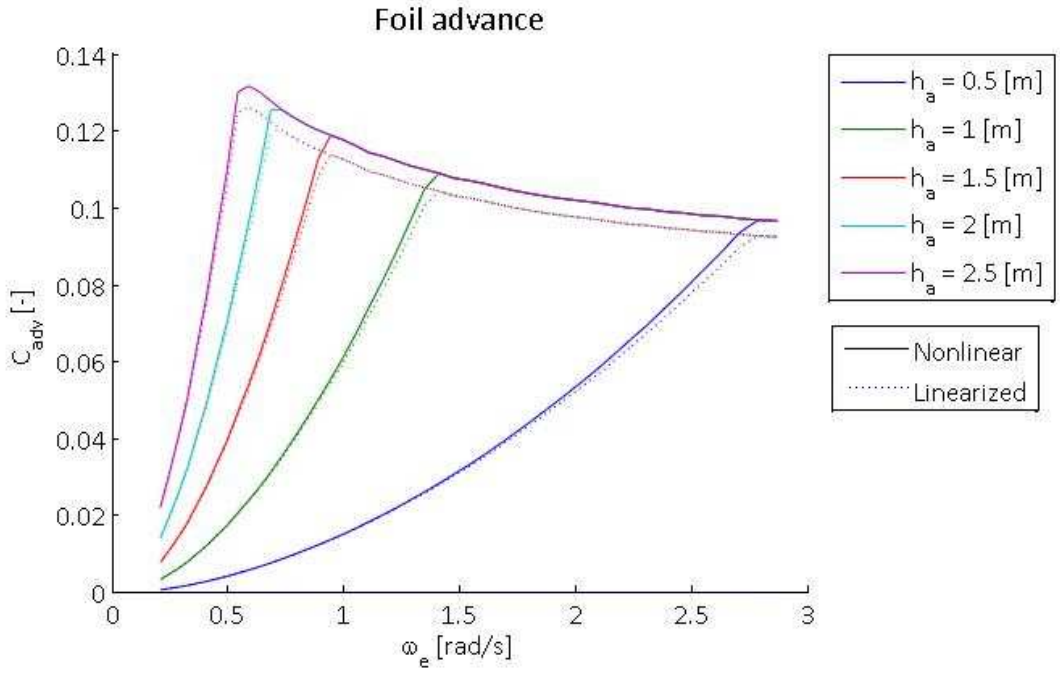

Figure 38: Case 3 advance coefficients for heave amplitudes from 0.5 to 2.5 [m]. Nonlinear and linear.

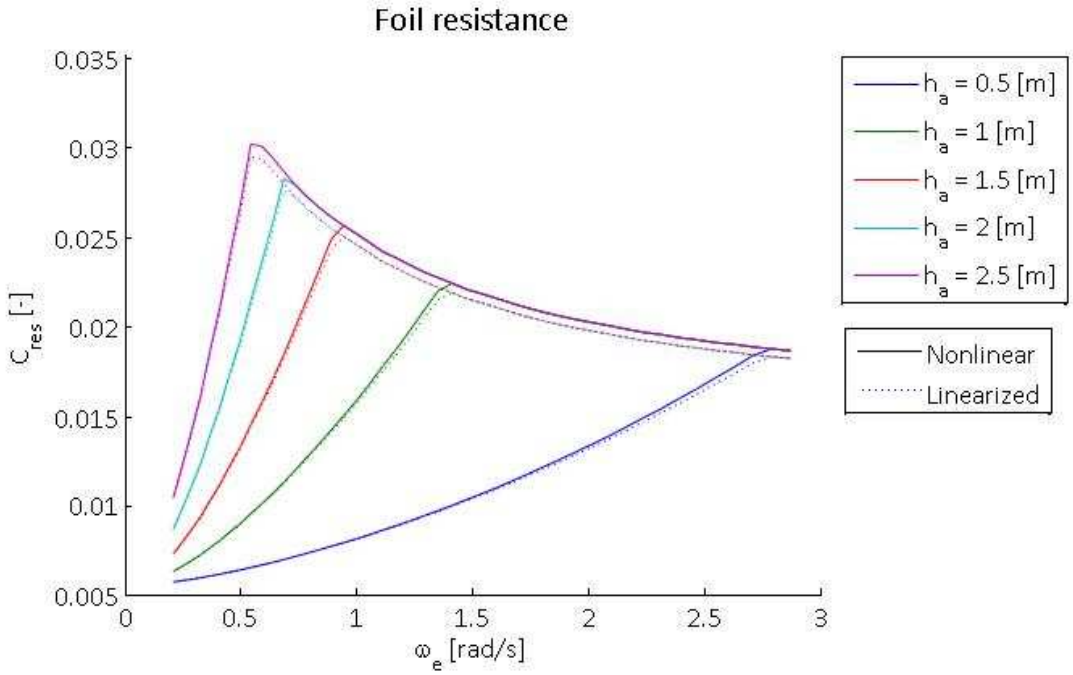

Figure 39: Case 3 resistance coefficients for heave amplitudes from 0.5 to 2.5 [m]. Nonlinear and linear.

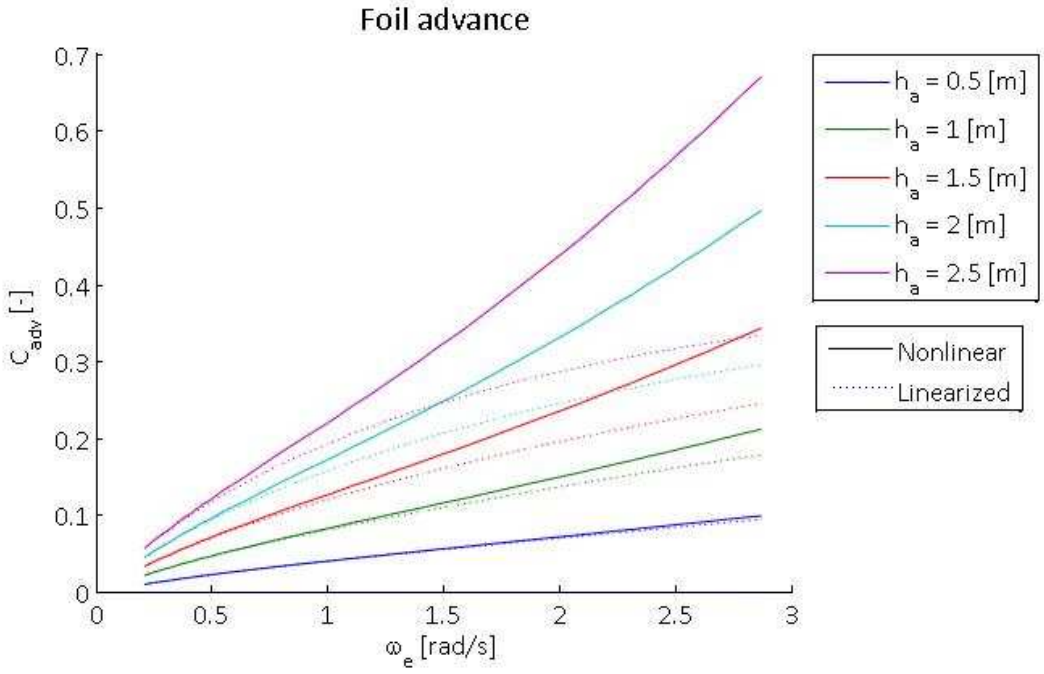

Figure 40: Case 4 advance coefficients for heave amplitudes from 0.5 to 2.5 [m]. Nonlinear and linear.

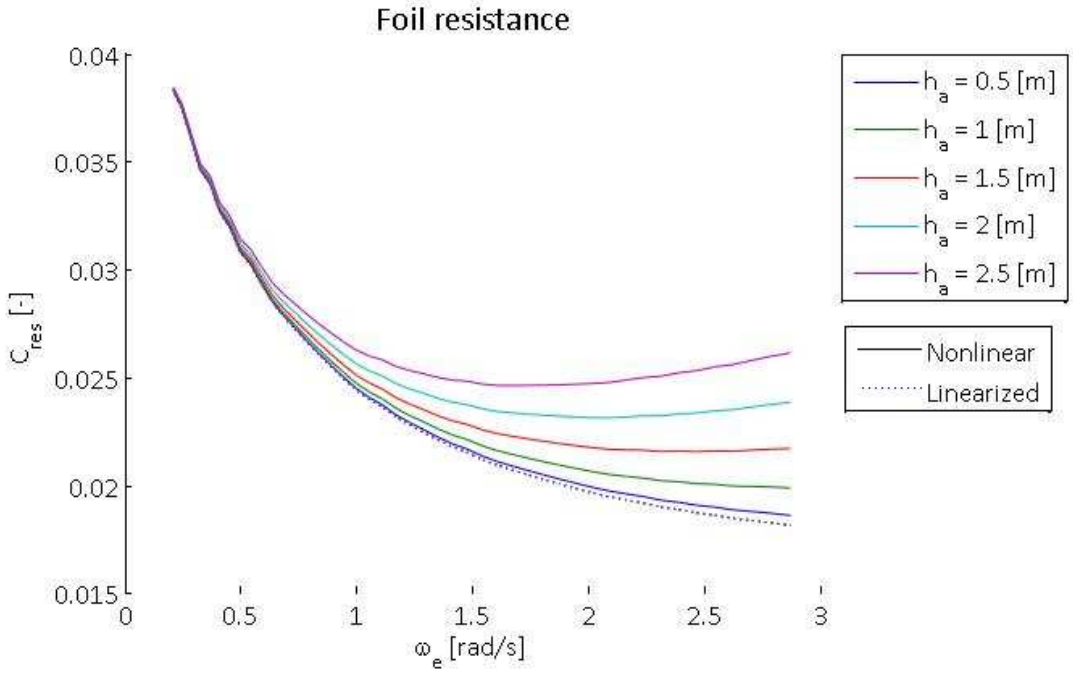

Figure 41